Cosmic Voids and Void Properties

A Thesis

Submitted to the Faculty

of

Drexel University

by

Danny C. Pan

in partial fulfillment of the

requirements for the degree

of

Doctor of Philosophy

June 2011

Dedications

This thesis is dedicated to my family and Shoshana.

Their love and support has made this possible.

Acknowledgments

I would like to acknowledge first and foremost my thesis advisor Michael S. Vogeley. His guidance and insight were critical in helping me throughout this journey. I would also like to acknowledge my thesis committee members David Goldberg, Gordon Richards, Ravi Sheth, and Luis Cruz-Cruz who kept me on track and whose constructive criticisms guided me in my research.

Table of Contents

List of Tables

List of Figures

Abstract

Cosmic Voids and Void Properties
Danny C. Pan
Dr. Michael S. Vogeley

The cosmic energy budget of the standard model of cosmology (ΛCDM) dictates that 72% of the Universe is Dark Energy (undetected, unknown), 23% Dark Matter (undetected, some candidates, largely unknown), and 4% baryons. Everything we have seen and detected including galaxies, stars, white dwarves, supernovae, and black holes make up just 4% of the known Universe. The predictions of ΛCDM has held up surprisingly well to various studies of the observable Universe, including Hubble Space Telescope observations of supernovae, Sloan Digital Sky Survey observations of the baryon acoustic oscillations, and Wilkinson Micro Anisotropy Probe studies of the cosmic microwave background. In my thesis, I test the predictions of ΛCDM on the large scale structure of the Universe, specifically voids. Using a void catalog generated from the Sloan Digital Sky Survey, I study the sizes and shapes of voids, the small scale distribution of void galaxies, and the distribution of Lyα (neutral hydrogen) clouds. I find that voids in the Universe have characteristic sizes and shapes based on cosmology, voids can be modeled as mini-universes where void galaxies are much less clustered than their wall counterparts, and the surprising result that Lyα clouds do not trace the large scale distribution of baryons or dark matter in the Universe.

Chapter 1

Introduction

1.1 Standard Model of Cosmology

The standard model of cosmology is the ΛCDM model. Combining data from baryon acoustic oscillations from the Sloan Digital Sky Survey [Percival et al., 2010] and priors on H_0 from Hubble Space Telescope observations, six fundamental standard model parameters were measured in the seven year Wilkinson Microwave Anisotropy Probe (WMAP) observations [Jarosik et al., 2011]. The parameters found are listed in Table 1.1.

Figure 1.1 and 1.2 from Percival et al. [2010] plots the error ellipses of a 2 parameter fit to data from WMAP, SN, and BAO. The best estimates for the parameters are $\Omega_m = 0.286 \pm 0.018$, and $H_0 = 68.2 \pm 2.2$ km s^{-1} Mpc^{-1}. Their results indicates $w \approx$ -1, showing a constant dark energy equation of state, and rules out curvature of space, $\Omega_k \approx 0$.

Table 1.1: Results from WMAP seven year cosmological parameter summary [Jarosik et al., 2011].

Description	Symbol	Result
Age of Universe	t_0	13.75 ± 0.13 Gyr
Hubble Constant	H_0	71.0 ± 2.5 km s^{-1} Mpc^{-1}
Baryon Density	Ω_b	0.0449 ± 0.0028
Dark Matter Density	Ω_c	0.222 ± 0.026
Fluctuation Amplitude at $8h^{-1}$ Mpc	σ_8	0.801 ± 0.030
Scalar Spectral Index	n_s	0.963 ± 0.014
Reionization Optical Depth	τ	0.088 ± 0.015

These parameters determine our best guess for the evolution of the Universe within which we reside. It dictates everything we know in the Universe stemming from the largest of scales, the general thermal isotropy of the cosmic microwave background, to medium scales, the distribution of galaxies and large scale structure in the Universe, to small scales, the abundance of radiation, matter, and baryons in the Universe. At each of these scales, astronomers seek to assess the predictions of the standard model of cosmology. We must understand how observations made fit into the grand predictions of the powerful model. We seek to test the ability of the model to properly predict the large scale structure in the Universe using optical observations of the galaxies.

1.2 Large Scale Structure

Redshift surveys of galaxies reveal a rich variety of large-scale structures in the Universe: clusters that span a few megaparsecs in radius, connected by filaments stretching up to many tens of megaparsecs, which in turn envelop vast underdense voids with radii of tens of megaparsecs. These large scale structures are described by Bond et al. [1996] as a Cosmic Web of material that reflects the initial density fluctuations of the early Universe. While historically most attention has been paid by astronomers to the dense clusters and filaments, it is the voids that fill most of the volume in the Universe. These underdense regions strongly influence the growth of large scale structure. The statistics and dynamics of cosmic voids and the properties of the few objects found within them provide critical tests of models of structure formation.

Observations of voids in the galaxy distribution have progressed as the depth, areal coverage, and sampling density of galaxy redshift surveys have improved. Rood [1988] reviews the paradigm shift that occured beginning in the mid-1970s as the focus shifted from the study of galaxy surface distributions to three-dimensional spatial distributions provided by redshift surveys, and the impact of this revolution on studies of voids. Joeveer et al. [1978] identified superclusters and voids in the distribution of galaxies and Abell clusters. Pencil beam surveys of the Coma/Abell 1367 supercluster [Gregory and Thompson, 1978] indicated large voids. Kirshner et al. [1981] discovered a void in the Bootes region of the sky that is 50 h^{-1} Mpc in diameter, several times larger than any previously observed. The Center for Astrophysics Redshift Survey [Huchra et al., 1983] and in particular its

extension to $m_B = 15.5$ [de Lapparent et al., 1986, Geller and Huchra, 1989] revealed that the large-scale structure of galaxies is dominated by large voids and the sharp filaments and walls that surround them. The Southern Sky Redshift Survey [da Costa et al., 1988, Maurogordato et al., 1992] found similar results. The Giovanelli and Haynes [1985] survey detailed the supercluster and void structure of the Perseus-Pisces region. The deeper Las Campanas Redshift Survey [Kirshner et al., 1991, Shectman et al., 1996] confirmed the ubiquity of voids in the large-scale distribution of galaxies. Comparison of optically-selected galaxy surveys with redshift surveys of infrared selected galaxies [Strauss et al., 1992, Fisher et al., 1995, Saunders et al., 2000, Jones et al., 2004] indicated that the same voids are found regardless of galaxy selection. The completed Two Degree Field Galaxy Redshift Survey (2dFGRS; Colless et al. [2001]) and Sloan Digital Sky Survey (SDSS; York et al. [2000], Abazajian et al. [2009]) now allow the most complete view to date of the detailed structure of voids.

A variety of methods have been used to compile catalogs of voids in both observations of galaxies or clusters and in simulations (using dark matter particles or mock galaxy catalogs). Detailed discussion of many of these methods is given by Colberg et al. [2008], who compare void finding techniques. For the purpose of finding voids in redshift survey observations, methods that are applicable to the distribution of galaxies include Kauffmann and Fairall [1991], El-Ad and Piran [1997], Aikio and Maehoenen [1998], Hoyle and Vogeley [2002], Neyrinck [2008], Aragon-Calvo et al. [2010]. Examples of applications of such methods to galaxy redshift surveys include analyses of the Southern Sky Redshift Survey [Pellegrini et al., 1989], the first slice of the Center for Astrophysics Redshift Survey [Slezak et al., 1993], as well as the full extension of the CfA Redshift Survey [Hoyle and Vogeley, 2002], the IRAS 1.2Jy and Optical Redshift Surveys [El-Ad et al., 1997, El-Ad and Piran, 1997, 2000], the Las Campanas Redshift Survey [Müller et al., 2000], the IRAS PSCz Survey [Hoyle and Vogeley, 2002, Plionis and Basilakos, 2002], the 2dFGRS [Hoyle and Vogeley, 2004, Ceccarelli et al., 2006, Tikhonov, 2006], and preliminary data from the SDSS [Tikhonov, 2007, Foster and Nelson, 2009].

The importance of cosmic voids as dynamically-distinct elements of large-scale structure is clearly

established by theory [Hoffman and Shaham, 1982, Hausman et al., 1983, Fillmore and Goldreich, 1984, Icke, 1984, Bertschinger, 1985, Blumenthal et al., 1992, Sheth and van de Weygaert, 2004, Patiri et al., 2006a, Furlanetto and Piran, 2006]. Linear theory predicts that the interior of the voids should reach a flat plateau and the boundaries of the voids should be quite sharp. Simulations of structure formation (e.g., Regos and Geller [1991], Dubinski et al. [1993], van de Weygaert and van Kampen [1993], Colberg et al. [2005]) demonstrate that large voids are caused by super-Hubble outflows that are nearly spherically symmetric out to near the edges of the voids. Tidal effects of clusters only become important for objects near the walls around voids. Simulations of the Cold Dark Matter model for structure formation indicate that the interiors of voids should include dark matter filaments and many low mass halos [Mathis and White, 2002, Benson et al., 2003, Gottlöber et al., 2003]. Identifying these structures is an important test of this model.

The properties of large voids in the distribution of galaxies may provide strong tests of cosmology. Ryden [1995], Ryden and Melott [1996] discuss the use of void shapes in redshift space as a cosmological test. More recent work examines voids as a probe of dark energy [Park and Lee, 2007, Lee and Park, 2009, Biswas et al., 2010, Lavaux and Wandelt, 2010] Comparison of voids at low and high redshift may provide a strong test of the ΛCDM model [Viel et al., 2008]. The abundance of cosmic voids is a critical probe for non-gaussianity in the initial conditions for structure formation [Kamionkowski et al., 2009, Chongchitnan and Silk, 2010, D'Amico et al., 1]. Beyond tests of the ΛCDM model, the properties of voids galaxies may even constrain alternative theories of gravity [Hui et al., 2009].

Mapping the voids is important both for studying large-scale cosmic structure and because they are a unique astrophysical laboratory for studying galaxy formation. Gravitational clustering within a void proceeds as if in a very low density universe, in which structure formation occurs early and there is little interaction between galaxies, both because of the lower density and the faster local Hubble expansion. Goldberg & Vogeley (2004) show that the interior of a spherical void with 10% of the mean density in a flat $\Omega_{matter} = 0.3$ $h = 0.7$ universe evolves dynamically like an $\Omega_{matter} = 0.02$, $\Omega_\Lambda = 0.48$, $h = 0.84$ universe.

Peebles [2001] describes the "void phenomenon": galaxies of all types appear to respect the same voids, in contrast to the prediction of CDM that low density regions should contain many low mass objects. Tikhonov and Klypin [2009] find, using comparison of voids and void galaxies in the local volume with high-resolution simulations, that the emptiness of voids is a problem for ΛCDM.

Voids are expected to harbor many low mass halos that are the ideal breeding grounds for faint galaxies; if the low mass halos predicted by CDM harbor luminous galaxies, then they should be optically visible. Optical observations have not revealed a large population of fainter galaxies in voids [Thuan et al., 1987, Lindner et al., 1996, Kuhn et al., 1997, Popescu et al., 1997], although the luminosity function in voids is shifted by about one full magnitude [Hoyle et al., 2005]. Tinker and Conroy [2009] contends the ΛCDM void phenomenon is due to a lack of understanding of assembly bias as galaxies form [Gao and White, 2007], but their model predicts a 5-magnitude shift in maximum galaxy luminosity. If void halos contain gas, but too few stars to be visible, then then their gas might be detected. To date, blind HI surveys have not detected such a population of HI rich but optically dark galaxies [Haynes, 2008]. Nearby Lyman-α clouds detected along lines of sight toward bright quasars show a strong preference for inhabiting the voids, but most of these clouds seem to be associated with galaxy structures (Pan et al., in preparation, chapter 6 below).

In contrast to a picture in which star formation in void halos is suppressed, our analyses of void galaxies in the SDSS DR2 and DR4 samples indicate that void galaxies are bluer and have higher specific star formation rates than galaxies in denser environments [Rojas et al., 2004, 2005, Park et al., 2007]. For the small number of dwarf galaxies in the earlier samples, we note even stronger trends with environment; at fixed morphology and luminosity, the faintest void galaxies are bluer and have higher star formation rates. Focusing on the blue population in voids, we find in these preliminary SDSS analyses, and von Benda-Beckmann and Müller [2008] find in 2dFGRS, that this blue population is not only more numerous, but also bluer and with higher star formation than in denser regions.

In Hoyle et al. [2005] we find a much fainter exponential cutoff in the luminosity function in voids ($\Delta M_r^* = 1.1$ mag) but no evidence for a change in the faint end slope between voids and "walls."

However, the uncertainties at faint magnitudes are quite large. We could not find a sub-population of "wall" galaxies selected by color, surface brightness profile, or $H\alpha$ equivalent width that matched both the faint end slope α and characteristic magnititude M_r^* of void galaxies. In Park et al. [2007] we again find that M^* monotonically shifts fainter at lower density. and that the faint end (measured only down to $M_r = -18.5$) slope varies significantly with density. These results are consistent with earlier analyses Grogin and Geller [1999, 2000]. These trends also persist into the "wall" regions closest to large voids [Ceccarelli et al., 2008]. When we estimate the mass function of void galaxies in SDSS and compare to the luminosity function [Goldberg et al., 2005] we find a good match with the predictions of the Press-Schechter model, thus the void galaxies appear to be nearly unbiased with respect to the mass.

While we see some clear trends, controversy persists in the literature as to whether or not galaxies in voids differ in their internal properties from similar objects in denser regions. For example, Rojas et al. [2004, 2005], Blanton et al. [2005], Patiri et al. [2006b], and von Benda-Beckmann and Müller [2008] reach varying conclusions that clearly depend on how environment is defined and which observed properties are compared. There is a marked difference between properties of the least dense 30% of galaxies (in regions with density contrast $\delta < -0.5$) and objects in deep voids which form the lowest density 10% of galaxies (in regions of density contrast $\delta < -0.8$, which is the theoretical prediction for the interiors of voids that are now going non-linear). All of these results, and the possible controversy among them, highlight the importance of building the largest possible, publicly released catalog of voids and void galaxies.

Lastly, for the purpose of examining the influence of environment on galaxy formation and evolution, it is important to make a distinction between void galaxies and isolated galaxies. Void galaxies are galaxies that reside within large scale void structures in the Universe. While this has an overall effect on the local environments of these void galaxies, it does not preclude galaxies from residing within small scale dense environments, or cloud-in-void as described in Sheth and van de Weygaert [2004]. Isolated galaxies are generally found by nearest neighbor distance measures typically on the scale of small (Mpc) nearby environments [Karachentsev et al., 2010, Karachentseva,

1973]; they do not necessarily reside in large scale voids.

1.3 Chapter Breakdown

This thesis has 7 main chapters. Chapter 1 introduces the state of cosmology and void research. Chapter 2 discusses the formation of the void catalog that is the basis of research on void properties and void content. Chapter 3 compares the void finding algorithm used in this thesis to other void finding algorithms, and it also discusses results of void finding from various cosmological models and simulations. Chapter 4 discusses the shapes of voids in the Universe and the implications of void ellipticity to the standard model of cosmology. Chapter 5 talks about the distribution of void galaxies, primarily the two point correlation function. Chapter 6 explores the distribution of baryons within voids, using Lyα clouds as a tracer for the intergalactic medium. Finally, chapter 7 concludes the thesis and discusses its major contributions as well as future work that can expand from results of the work in this thesis.

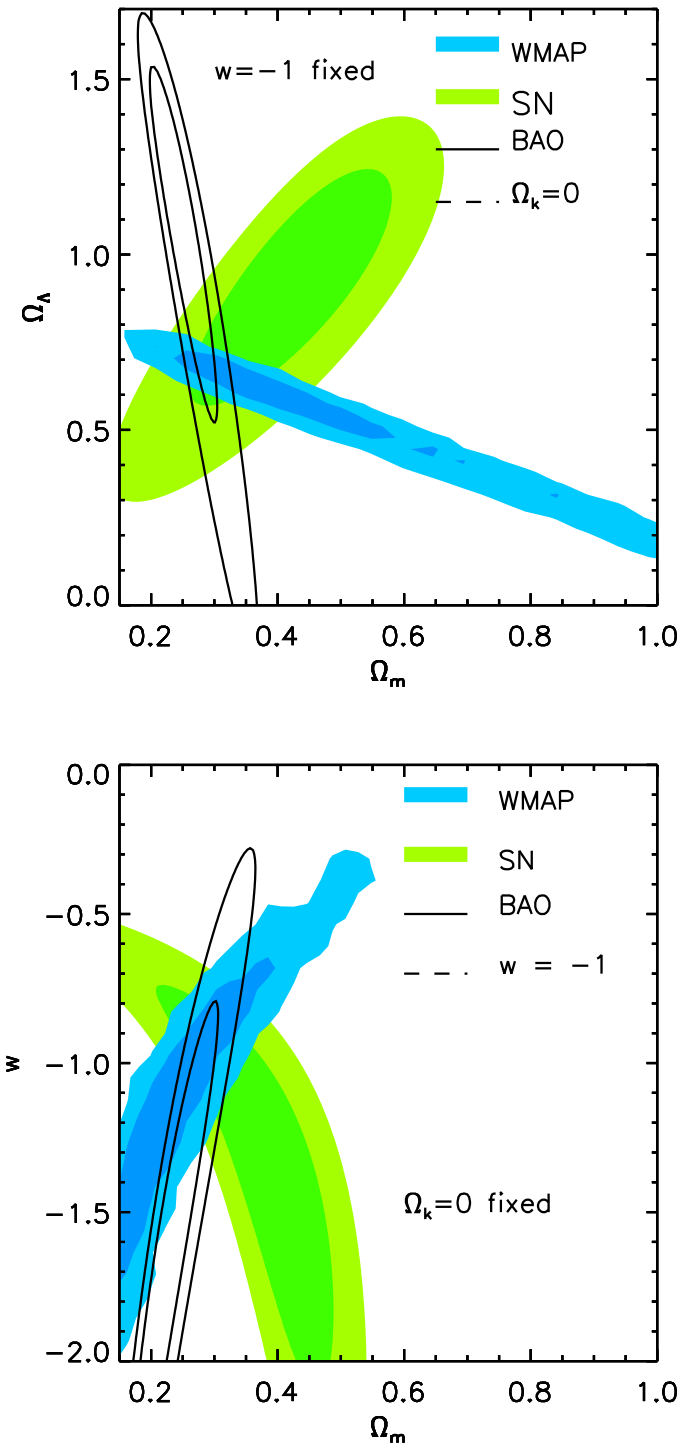

Figure 1.1: Top: Constraints comparing Ω_m and Ω_Λ from Percival et al. [2010] using error ellipses from WMAP, SN, and BAO assuming w = -1. Bottom: Error ellipses for Ω_m versus w. The plots indicate that w $\approx$ -1, and independently, all 3 measurements agree on similar values for cosmological parameters.

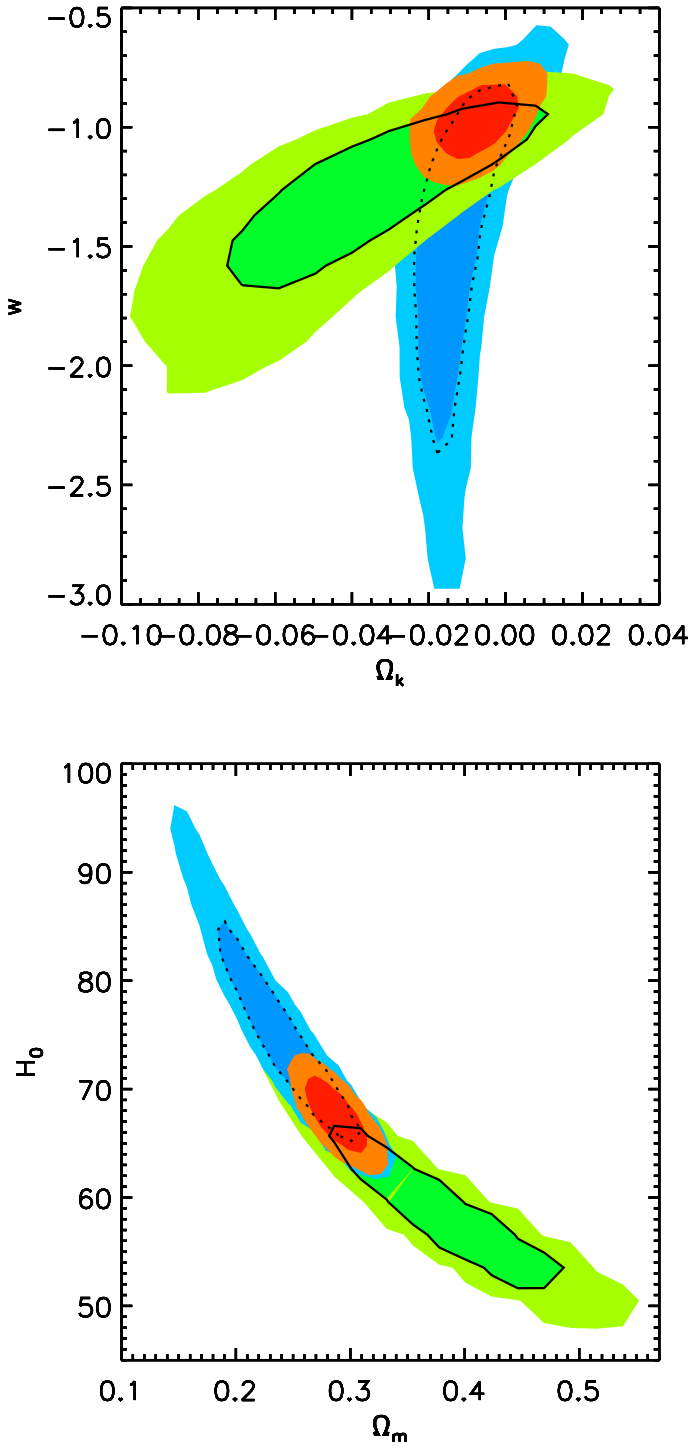

Figure 1.2: Top: Percival et al. [2010] find very good constraints on w ≈ -1 and $\Omega_k \approx 0$. Bottom: SDSS BAO measurements lie exactly between the error ellipses of SN and WMAP measurements, allowing them to constrain Ω_m and H_0 to very precise values.

Chapter 2

Void Catalog

A void catalog must be generated for the purpose of allowing precision cosmological tests with voids and more accurate tests of galaxy formation theories. We utilize a galaxy based void finding algorithm, "VoidFinder" [Hoyle and Vogeley, 2002], to identify voids in the final galaxy catalog from SDSS (DR7). This void finding technique is shown to accurately identify large-scale cosmic voids with properties similar to those predicted by gravitational instability theory. Section 2.1 describes the VoidFinder algorithm. Section 2.2 describes the SDSS data used for this research. Section 2.3 presents results on the various properties of the voids found. Sections 2.4 and 2.5 describe several methods used to test the robustness of the method.

2.1 VoidFinder

VoidFinder is a galaxy-based void finding algorithm that uses redshift data to find statistically significant cosmic voids. VoidFinder is based on the original VoidFinder method devised by El-Ad and Piran [1997] and implemented by Hoyle and Vogeley [2002], and uses a nearest neighbor algorithm on a volume limited galaxy catalog. This approach is highly effective in identifying large voids of density contrast $\delta \leq -0.9$ and radius $R > 10h^{-1}$Mpc. The method is robust when applied to different surveys that cover the same volume of space (we have applied VoidFinder to IRAS PSCz, CfA2+SSRS2, 2dF, SDSS, 6dF and compared overlaps; see Hoyle and Vogeley [2002, 2004]). Our

tests on cosmological simulations demonstrated that this method works in identifying voids in the distributions of both simulated galaxies and dark matter [Benson et al., 2003].

VoidFinder is applied to volume limited galaxy samples. The galaxies are initially classified as wall or field galaxies. A field galaxy is a galaxy that may live in a void region whereas wall galaxies lie in the cosmic filaments and clusters. The distance parameter d for determining whether a galaxy is a wall or field galaxy is based on the third nearest neighbor distance (d_3) and the standard deviation of the distance (σ_{d_3}):

$$d = d_3 + 1.5\sigma_{d_3}$$

In our galaxy sample, this selection parameter is $d > 6.3h^{-1}$ Mpc for field galaxies. With this value of d and choice of $M_{lim} = -20.09$ (SDSS r-band Petrosian magnitude), all field galaxies reside in underdense regions with density contrast $\delta\rho/\rho < -0.47$. Voids are expected to be significantly underdense, containing approximately 10% of the cosmic mean density. Near the edges of the voids, the density is expected to rise very sharply, drastically going from 20% of the mean density to 100%. Using this criterion for the edges of voids, it is expected that the distance criterion for void galaxies will depend on the density at the edge of the void and the spatial correlation of galaxies in voids and the fact that we are sitting on a galaxy. If we assume that the density at the edge of a void is 20% of the mean, then the expected density ρ around a galaxy near the void edge can be calculated as

$$\rho(r)/\bar{\rho} = (0.2)(\xi(r) + 1) \tag{2.1}$$

where $\xi(r)$ is the two point autocorrelation function of the galaxy sample. The average density in a sphere of radius R around a galaxy near the void edge is therefore

$$\rho(R)/\bar{\rho} = (0.2)(\bar{\xi}(r) + 1) \tag{2.2}$$

where $\bar{\xi}(R)$ is the average value in a sphere of radius R. Over the scales of interest here, the redshift-

space correlation function for galaxies in our volume-limited sample can be approximated by a power law,

$$\xi = (s/s_0)^{-\gamma} \tag{2.3}$$

with $s_0 = 7.62 \pm 0.67$ and $\gamma = 1.69 \pm 0.1$. Using these values, we can determine the values of R_{20}, the radial distance from a void galaxy where we would expect to encounter 20% of the mean density, and $\delta_{d=6.3}$, the expected underdensity of a void if its third nearest neighbor is found at a distance of 6.3 h^{-1} Mpc away. We find

$$R_{20} = 4.8^{+0.62}_{-0.74} h^{-1} Mpc \tag{2.4}$$

$$\delta_{d=6.3} = -0.88 \tag{2.5}$$

We expect that at the edges of the voids $\delta = -0.8$, and in the centers of the voids $\delta = -0.9$. Thus, our choice for the value of d allows us to pick out void galaxies conservatively, selecting mostly galaxies that only live near the centers of the voids and not allowing void regions to grow into the nonlinear regime. All galaxies with third nearest neighbor distance $d_3 > 6.3h^{-1}$ Mpc are considered to be potential void galaxies and are removed from the galaxy sample, leaving us a list of wall galaxies.

We map out the void structure by finding empty spheres in the wall galaxy sample that remains. Wall galaxies are gridded up in cells of size 5 h^{-1} Mpc, which allows us to find all voids larger than 8.5 h^{-1} Mpc in radius. All empty cells are considered to be the centers of potential voids. A maximal sphere is grown from each empty cell, but the center of the maximal sphere is not confined to the initial cell. Eventually the sphere will be bound by 4 wall galaxies. There is redundancy in the finding of maximal spheres, but this is useful to define non-spherical voids.

The sample of empty spheres now represents our potential void regions. We sort the empty spheres by size starting with the largest. The largest empty sphere is the basis of the first void region. If there is an overlap of $> 10\%$ between an empty sphere and an already defined void then

the empty sphere is considered to be a subregion of the void, otherwise the sphere becomes the basis of a new void. There is a cutoff of 10 h^{-1} Mpc for the minimum radius of a void region as we seek to find large scale structure voids that are dynamically distinct and not small pockets of empty space created by a sparse sample of galaxies. Any field galaxies that lie within a void region are now considered void galaxies. For further details of this implementation VoidFinder algorithm see Hoyle and Vogeley [2002, 2004].

2.2 Data: SDSS DR7

We use the SDSS Data Release 7 (DR7) [Abazajian et al., 2009] sample of galaxies. The SDSS is a photometric and spectroscopic survey that covers 8,032 square degrees of the northern sky. Observations were carried out using the 2.5m telescope at Apache Point Observatory in New Mexico in five photometric bands: u, g, r, i, and z [Fukugita et al., 1996, Gunn et al., 1998]. Follow up spectroscopy was carried out for galaxies with Petrosian r band magnitude $r < 17.77$ after each photometric image was reduced, calibrated and classified [Lupton et al., 2001, 1999, Strauss et al., 2002].

Spectra were taken using circular fiber plugs with an angular size of approximately 55 arc seconds. If two galaxies were closer than this, we could only obtain the spectra of one; the other object is omitted unless there is plate overlap. Blanton et al. [2003] addresses the issue of fiber collisions by assessing the relation between physical location of the galaxy and photometric and spectroscopic properties and assigns a redshift to the object missed by SDSS.

We use the Korea Institute for Advanced Study Value-Added Galaxy Catalog (KIAS-VAGC) [Choi et al., 2010]. Its main source is the New York University Value-Added Galaxy Catalog (NYU-VAGC) Large Scale Structure Sample (brvoid0) [Blanton et al., 2005] which includes 583,946 galaxies with $10 < r \leq 17.6$. After removing 929 objects that were errors, mostly deblended outlying parts of large galaxies, including 10,497 galaxies excluded by SDSS but that were part of UZC, PSCz, RC3, or 2dF, and also including 114,303 galaxies with $17.6 < m_r < 17.77$ from NYU-VAGC (full0), there is a total of 707,817 galaxies. This catalog offers an extended magnitude range with high completeness from $10 < r < 17.6$. There are 120,606 galaxies with $z < 0.107$ and $M_r < -20.09$ in

the volume limited sample used for void finding.

2.3 Measurement of Void Properties

We identify 1,054 voids in SDSS DR7 with minimum radius r = 10 h^{-1} Mpc. The largest voids are 30 h^{-1} Mpc in effective radius, where the volume of the void region is equal to the volume of the sphere with radius r_{eff}, and the median effective void radius is 17 h^{-1} Mpc. The voids cover 62% of the volume in the sample, and contain 7% of the volume limited galaxies. These results are similar to previous findings by El-Ad and Piran [1997] using a much smaller observation volume. We also identify 79,947 void galaxies with SDSS spectra that lie within the voids in the $r < 17.6$ magnitude limited catalog, which corresponds to 11.3% of the magnitude limited galaxies.

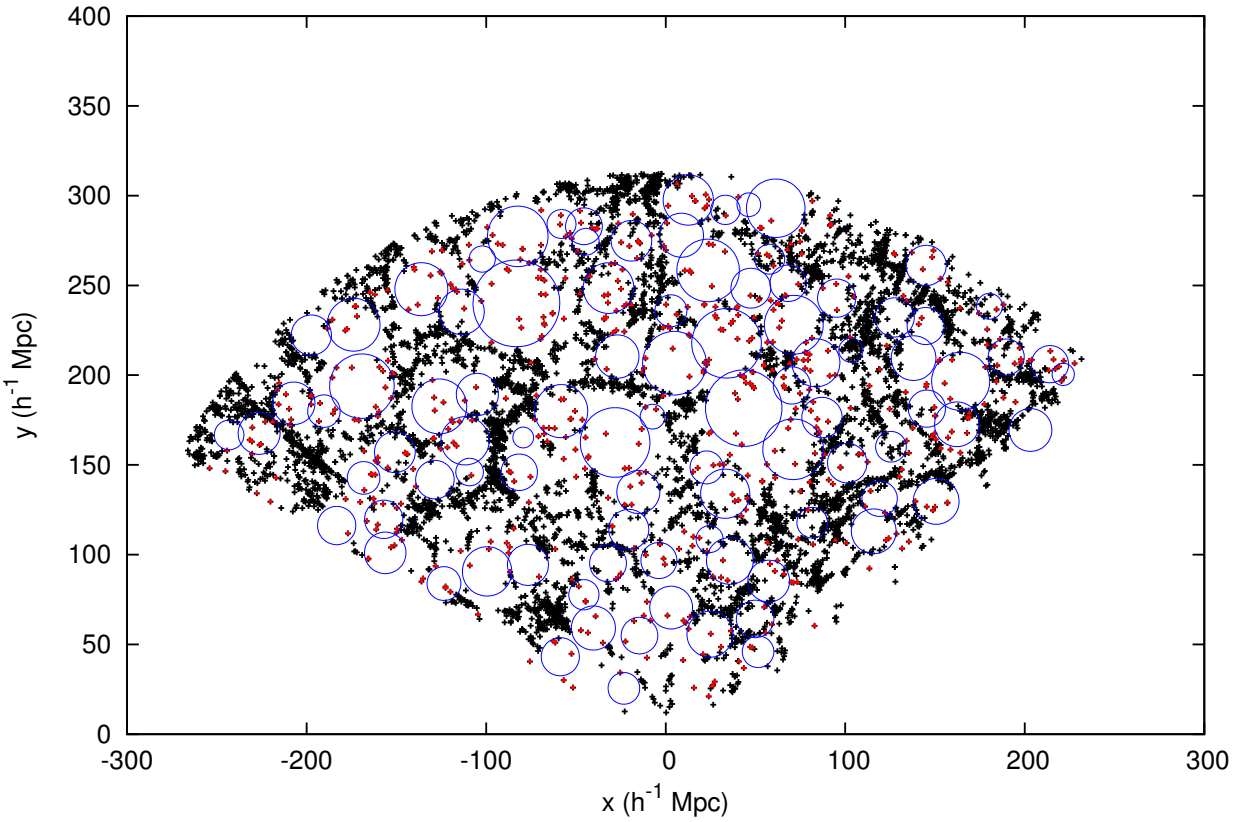

Figure 2.1: 10 h^{-1} Mpc thick slab through the middle of the largest void at RA = 226.52960, DEC = 60.41244. Locations of galaxies ($M_r < -20.09$) are shown with *, and the locations of void galaxies are shown with +. The circles show the intersection of the maximal sphere of each void with the midplane of the slab.

2.3.1 Void Sizes

Figure 2.1 shows a redshift slab of 10 h^{-1} Mpc in thickness going through the center of the largest maximal sphere detected by VoidFinder. The intersections of the plane with all maximal spheres of void regions are shown. It can be seen that even with just the maximal spheres, a large volume of space is underdense and galaxies cluster strongly in large filament-like structures. Figure 2.2 (top) shows the radius histogram based on the largest maximal sphere that defines the void region. It can be seen that the majority of the voids are small in size with a few very large void regions. Figure 2.2 (bottom) shows the effective radius of the individual void regions. It is important to remember that the maximal spheres are limited to $r > 10h^{-1}$ Mpc and thus only spherical void regions are found around 10 h^{-1} Mpc in effective radius. Most voids are not spherical and the skew in the effective radius histogram reflects the ellipticity of the voids.

In figure 2.3 we see that the majority of volume occupied by voids are occupied by moderately sized voids with 15 ¡ r_{eff} ¡ 25 h^{-1} Mpc. Figure 2.4 shows the cumulative volume enclosed by voids as a function of the void radii. Even though a large number of voids are smaller in size, the actual volume distribution indicates that there is a preferred size for large scale structure in the Universe. This is consistent with observations starting with the early redshift surveys to SDSS today. As indicated in Shandarin et al. [2006], void sizes are largely determined by the cosmology.

2.3.2 Radial Density Profiles

The radial density profiles of the cosmic voids show that voids are significantly underdense, having less than 10% of the average density all the way out to the very edge of the voids. The comparison of density is typically done by calculating the δ parameter. δ is defined as follows.

$$\delta = (\rho - \bar{\rho})/\bar{\rho} \tag{2.6}$$

δ = -1 would mean that the region is completely empty, and $\delta = 0$ implies that we are at the average density of the Universe. Figure 2.5 (top) shows the stacked radial density profile of voids.

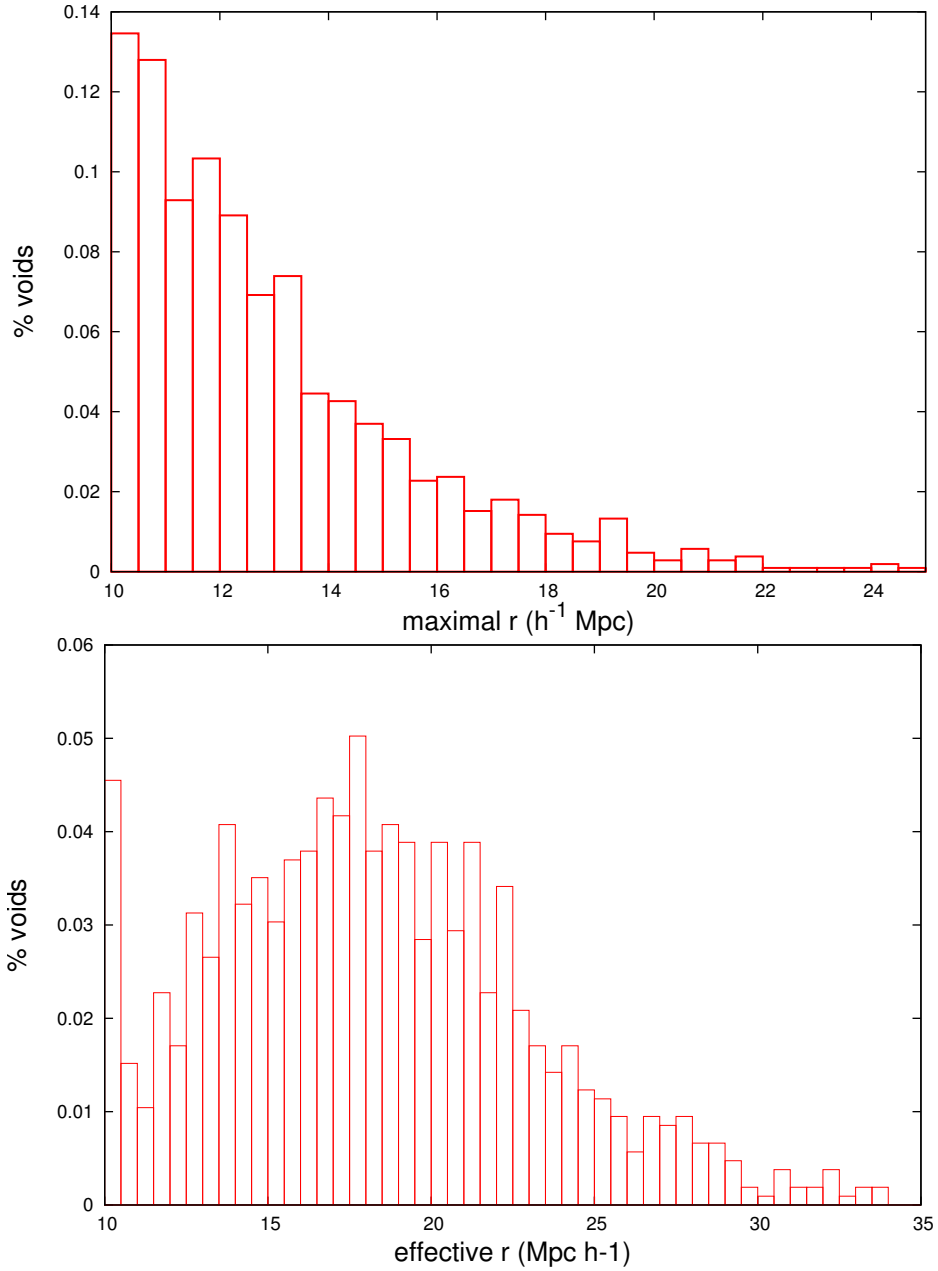

Figure 2.2: Distribution of void sizes as measured by the radius of the maximal enclosed sphere (top panel) and by effective radius (bottom panel). There is a cutoff of 10 h^{-1} Mpc for the holes that make up the voids and voids with r_{max} near this cutoff make up the majority of the void sample by number. The shift in the void distribution from the top to bottom panels indicates that the the void volumes are not well described by their maximal spheres; most voids are elliptical. Thus, the lack of small voids in the bottom panel is attributed to their ellipticity.

The density is calculated from the volume enclosed to the given effective radius of the void. Figure 2.5 (bottom) shows a similar stacked radial density profile of the voids. However, the density is now

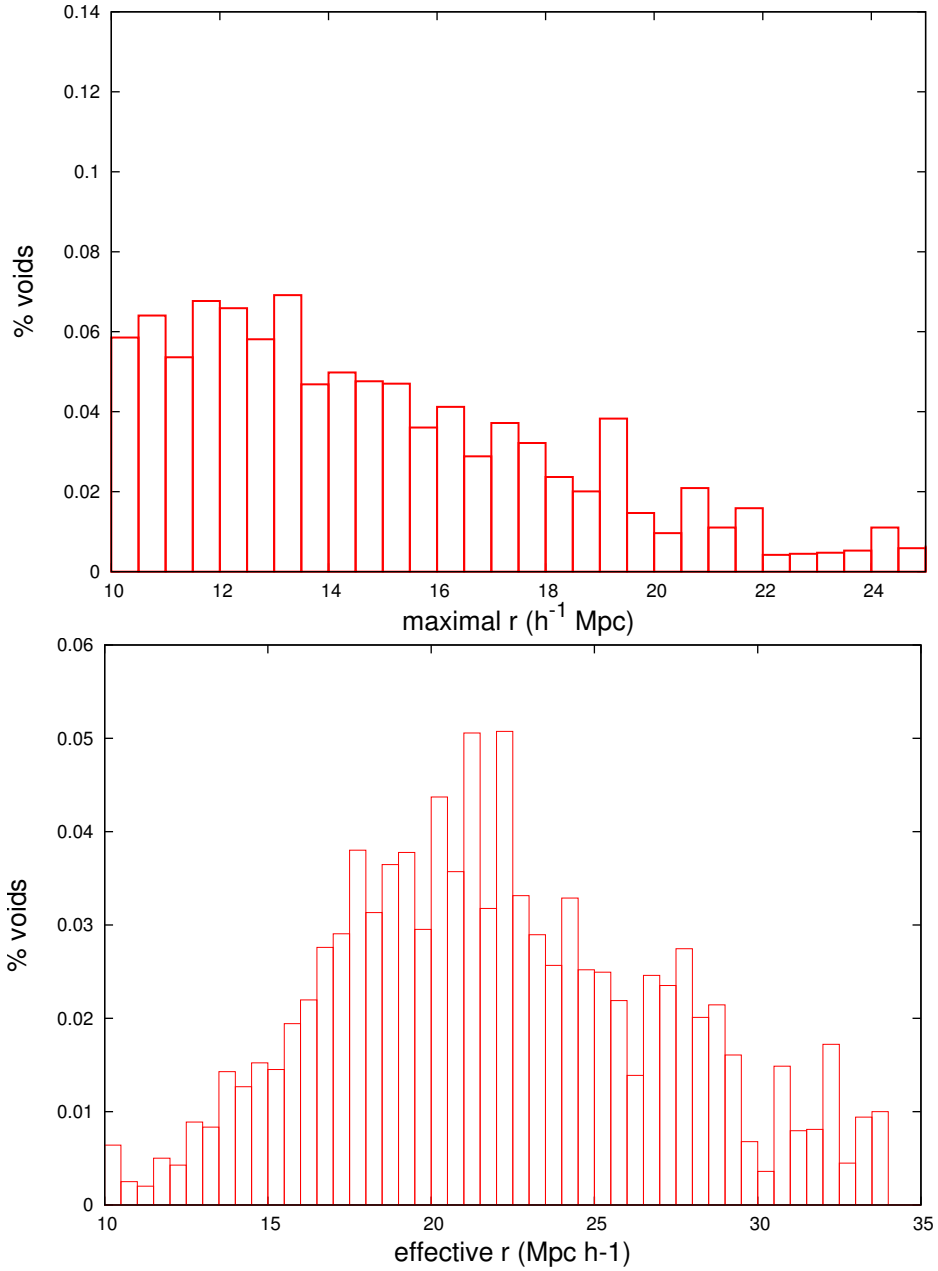

Figure 2.3: Distribution of void sizes as a percentage of the volume occupied by the voids. As in Figure 2, the top panel sorts voids by their maximal sphere radii, on the bottom by their effective radii. Large voids occupy most of the volume with 50% of the volume occupied by voids with maximal sphere $r > 13.8h^{-1}$ Mpc, and void size effective $r > 17.8h^{-1}$ Mpc. Note the peak of the radius histogram distribution around $22h^{-1}$ Mpc, the typical size of voids in the Universe.

calculated for spherical annuli. It can be seen that the walls of the voids are quite sharp, quickly growing from 10% of the average density to 100%, and the voids are very well defined in terms of

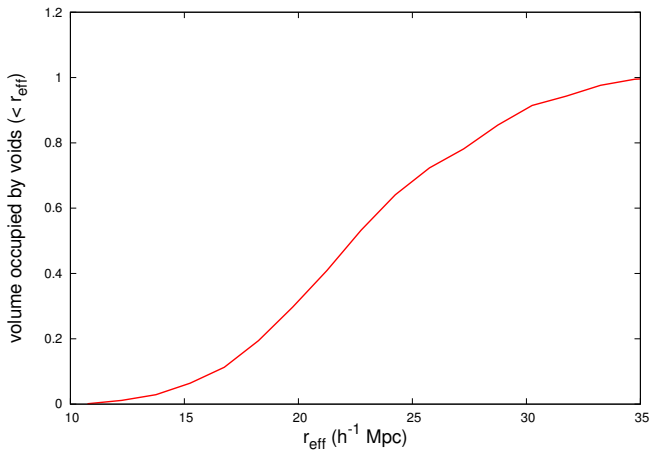

Figure 2.4: Cumulative volume enclosed by voids with r_{eff}. Small voids make up a very small fraction of the overall volume filled by voids in the Universe. Most of the volume is determined by middle to large sized voids as seen in Figure 3.

their density contrast with the outside Universe. It is clear then that these voids are distinct features of the Universe. A comparison with linear gravitation theory (Figure 2.7, reproduced from Sheth and van de Weygaert [2004]) shows the same "bucket shaped" radial density profile (see also Figure 4 of Fillmore and Goldreich [1984]).

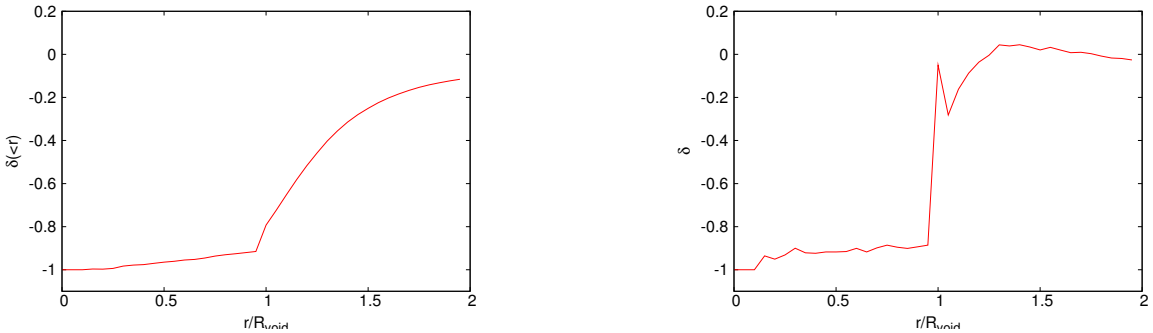

Figure 2.5: The average radial density profile of all 1,054 voids in the void catalog after scaling the profiles by R_{void} and stacking. The figure on the top is the profile of the enclosed volume, and the figure on the bottom is the profile in spherical shells. In both figures, there is a very sharp spike near the edges of the voids. The steep rise in the density contrast is because walls of voids are well defined. The peak at the edge of the void in the spherical shelss may be a feature of the density of the sample.

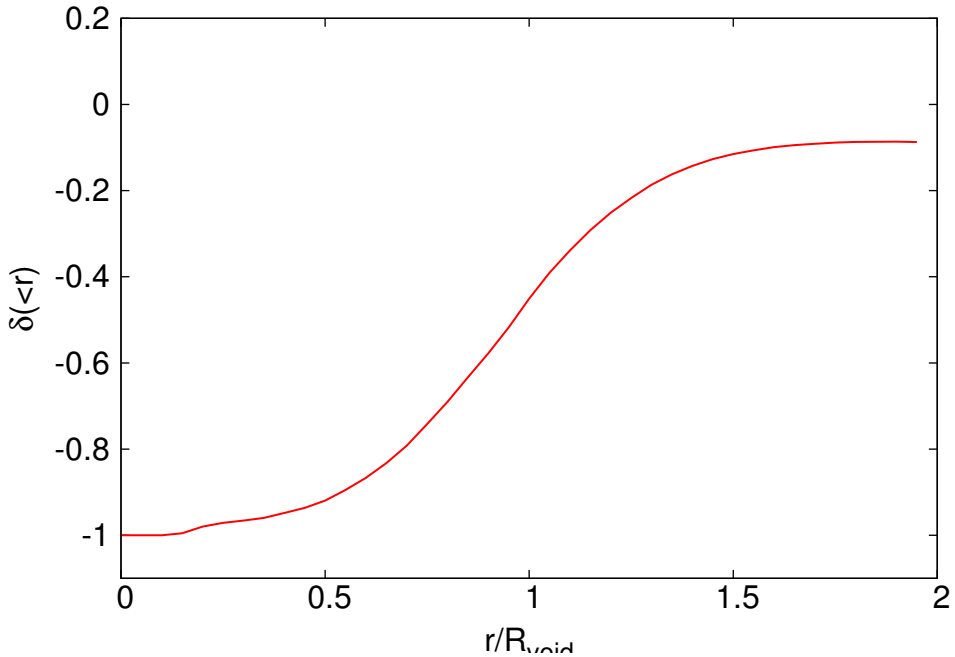

Figure 2.6: The average radial density profile of all 1,054 voids in the void catalog as a function of the effective radius. The slope of the radial densities measured near the edges of voids is smoother because we are probing regions possibly contaminated with wall galaxies if the voids are elliptical.

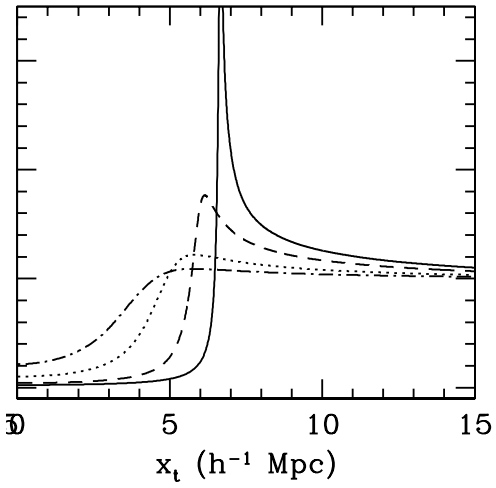

Figure 2.7: Radial density profile (spherical annulus) as predicted by linear gravitation theory [Sheth and van de Weygaert, 2004]. The different curves correspond to different epochs of evolution, with the tallest peak representing $z = 0$.

2.3.3 Void Galaxies

In our SDSS DR7 galaxy catalog, there are 708,788 galaxies. In our $M < -20.09$ volume limited galaxy catalog, there are 120,606 galaxies, with 8,046 of them falling inside voids, approximately 7%. There are 79,947 (11%) void galaxies that lie in void regions from the magnitude limited catalog with $z < 0.107$. Properties of these void galaxies will be discussed in a later paper.

2.4 Tests: Volume Limited Cuts

In this section, we study the effect of changing the absolute magnitude cut on the voids found by VoidFinder. For absolute magnitudes brighter than $M_r = -20.09$, we use the same redshift cut while eliminating galaxies that fall under the absolute magnitude cut of $-20.2, -20.3... - 20.6$. For absolute magnitudes dimmer than $M_r = -20$, we use a redshift cut of $z = 0.087$, which corresponds to a limiting absolute magnitude of -19.5, and apply VoidFinder to samples with magnitude limits of $-19.5, -19.6... - 20.1$. It can be seen that as we slightly shift the absolute magnitude limits the void distribution remains similar, although there are trends that voids generally grow in size with brighter absolute magnitude cuts and voids get smaller in size with dimmer absolute magnitude cuts, as expected for changes in the sampling density of galaxies. We find qualitatively different behavior as we examine extremely different samples (L*$\pm$0.5 magnitude), where we start to observe the effects of merging and splitting of voids.

Figure 2.8 shows that the void regions found by VoidFinder are consistent for almost all large voids. The only significant discrepancy arises from smaller voids that are introduced in sparser samples of the data. Figure 2.9 shows that the radial density profiles still show the "bucket shaped" feature.

Thus, the voids we find are not very sensitive to the absolute magnitude cut nor to the volume of our sample. SDSS DR7 provides a sufficiently contiguous three dimensional volume for void finding purposes. These voids found by VoidFinder should be considered significant large scale underdensities.

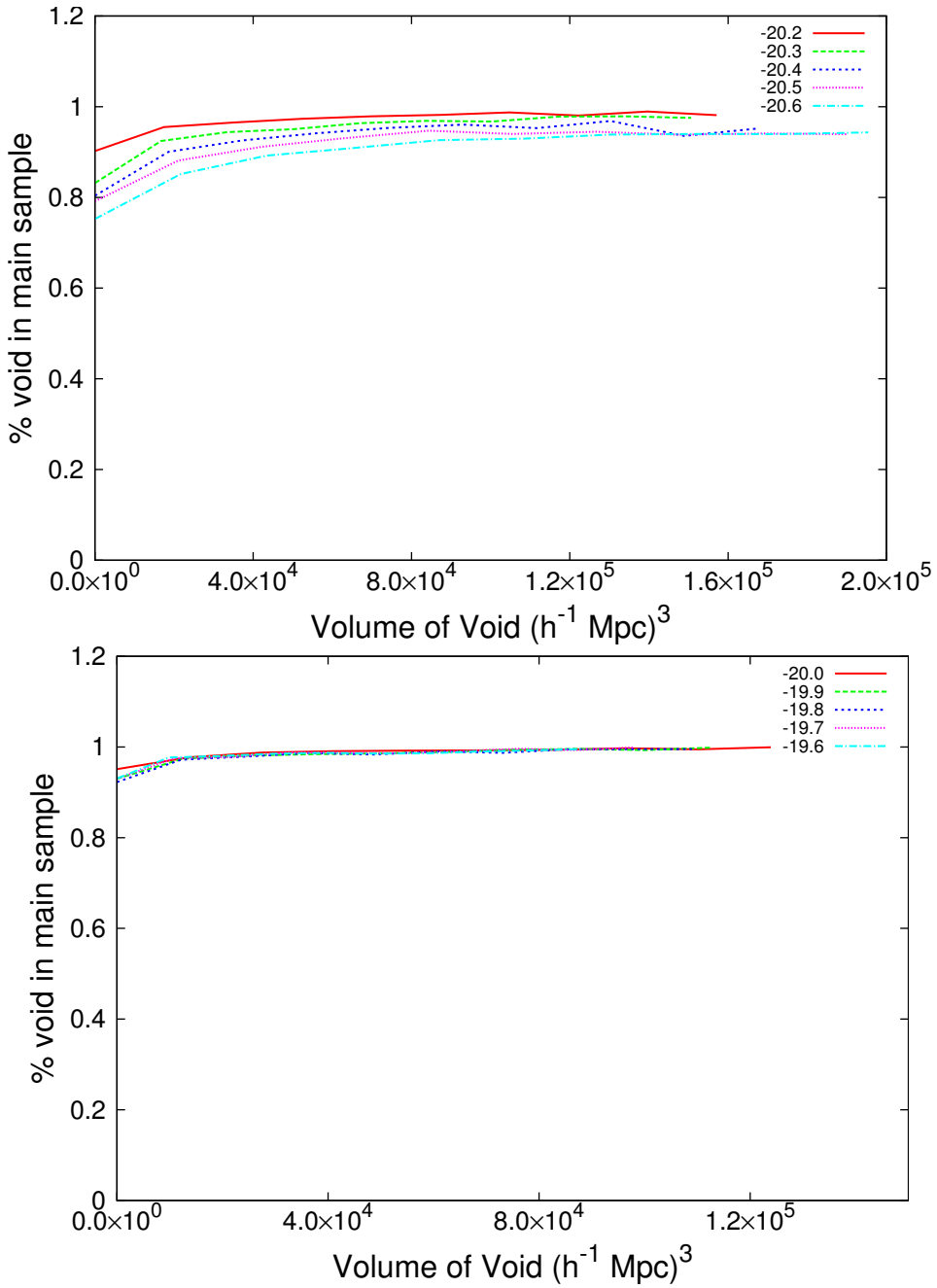

Figure 2.8: Overlap fraction for galaxy samples with redshift cut $z = 0.107$ (top), and $z = 0.087$ (bottom) with magnitude given in the figure compared to the void catalog sample ($M_{lim} = -20.09$). The y-axis shows the fraction of the void volume that is also considered void in the main sample as a function of the void volume. It can be seen that the large significant voids are consistently identified regardless of the volume limited cut.

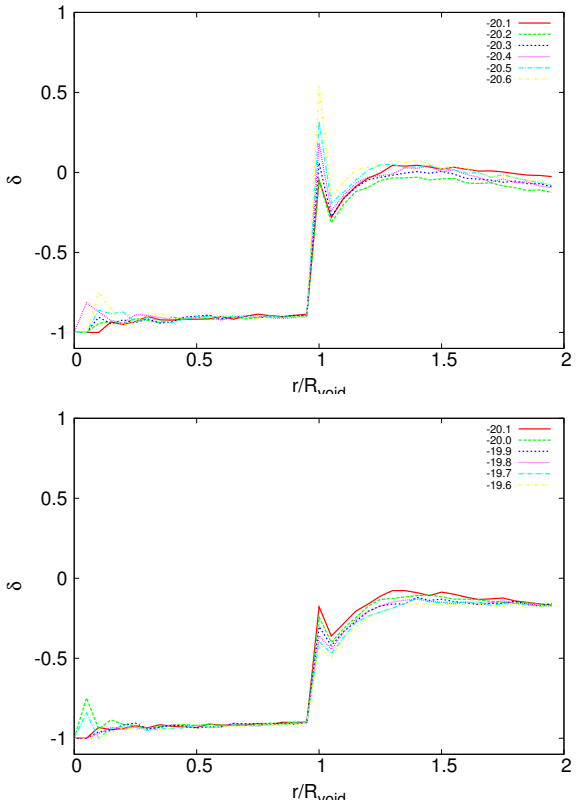

Figure 2.9: Radial density profile (enclosed volume) for galaxy samples with $-20.6 < M_r < -20.1$ (top), and $-20.1 < M_r < -19.6$ (bottom). The only difference between the profiles is the height of the peak at the edge of the voids. This is due to the different number density of galaxies in the sample used to determine voids. The bucket shaped behavior at the walls of the voids is consistent with Sheth and van de Weygaert [2004] in Figure 2.7.

2.5 Tests: Mock Data

We test the void finding algorithm on a set of mock galaxy catalogs to analyze the effects of the boundary conditions as imposed by SDSS, the effectiveness of studying large scale 3D structure in the finite volume of SDSS, as well as to test Λ-CDM predictions of the properties of voids. The mock catalog used is a dark matter only model [Skibba and Sheth, 2009] enclosed in a cube with sides 480 h^{-1} Mpc. The luminosity function and luminosity weighted correlation functions of the mock catalogue are fit to SDSS as described by Skibba et al. [2006], using halo occupation constraints from Zheng and Weinberg [2007]. The simulation parameters, in particular Ω_M and σ_8 are given in Yoshida et al. [2001].

We test VoidFinder on the mock sample using two different methods. First, the SDSS mask

is applied to the mock sample so that the geometries of the samples are the same; the results of this should mimic that of SDSS DR7. The SDSS geometry mock catalog contains 98,186 galaxies covering a volume of 2.2×10^7 Mpc^3 in the volume limited sample. Second, a cube is selected with volume similar but greater than the SDSS geometry sample. The cube geometry mock catalog contains 119,076 galaxies covering a volume of $2.7 \times 10^7 Mpc^3$.

2.5.1 Mock Results

There are 1,006 voids and 6,228 void galaxies in the SDSS geometry mock catalog. There are 1,246 voids and 7,881 void galaxies in the cube geometry mock catalog. The void volume fraction in the SDSS volume cut is 66.5%, and 69.3% in the cube volume cut. We observe that the geometry of SDSS plays a role in determining the overall void volume fraction, and if a SDSS geometry is considered in a mock sample, the volume fraction (66.5%) is approximately the same as the observed SDSS void volume fraction (62%). The effective radius histogram of voids found in the mock samples in Figure 2.11 shows no significant changes in the sizes of voids found in the mock samples. The radial density profile in Figure 2.10 shows that the interiors of the voids are similarly empty as well. The void size and density profile results of the mock samples agree with observational data. However, there does seem to be a difference in the number of void galaxies found by VoidFinder which will be discussed in a separate paper.

	SDSS	SDSS mock	mock cube
# voids	1,054	1,006	1,246
voids/volume	0.000048	0.000046	0.000046
# void gals	8,046	6,228	7,881
# void gals/volume	0.00037	0.00028	0.00029

2.6 Void catalog release

We have made this void catalog publicly available for future studies of voids. Included in the catalog are three separate interpretations of void regions. The first catalog consists of the maximal spheres of each unique void region. This is the largest hole in each void region in the shape of a sphere.

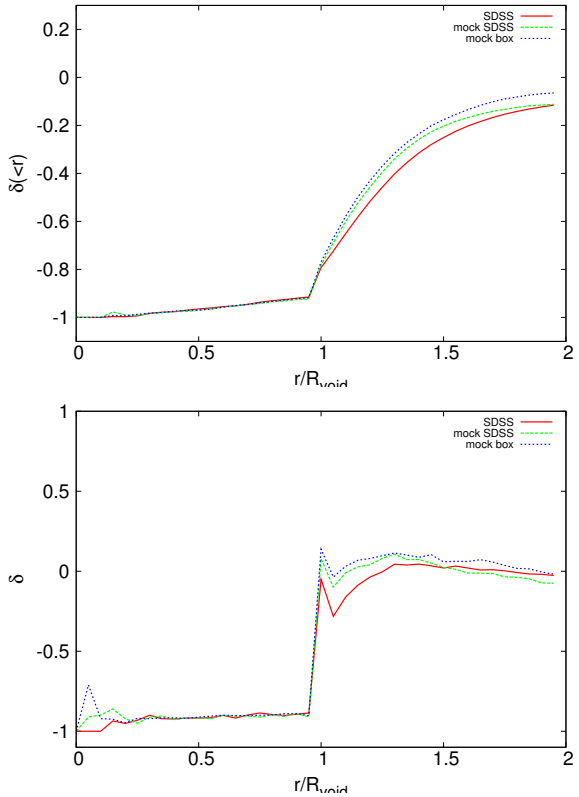

Figure 2.10: Comparison of radial density profiles of voids in SDSS DR7 and simulations (top panel shows enclosed density, bottom panel shows density in spherical shells). The density profiles within the voids are nearly identical in all cases. The simulations show a slight tendency toward larger density just outside the void boundary.

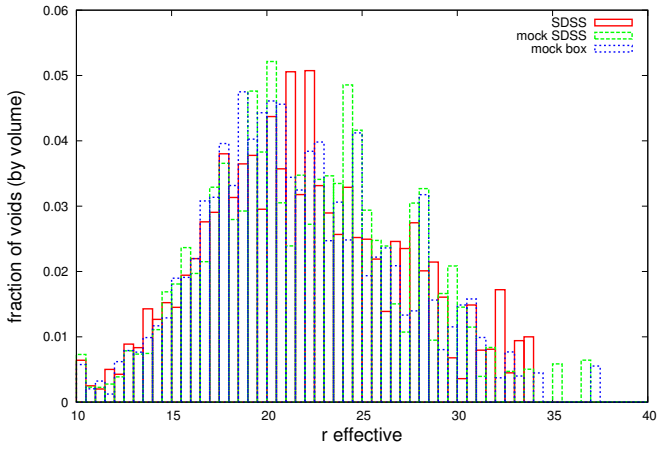

Figure 2.11: Distribution of void filling factor as a function of effective radius for voids found in SDSS DR7 and simulations. The distribution of void sizes found in the mock catalogs are nearly identical to those found in SDSS. The same size voids fill most of the volume.

This catalog is particularly useful for studying vast spherical underdense regions of the Universe. These spheres often depict the most underdense regions and galaxies near the centers of these voids are living in the most underdense large scale environments. The second catalog consists of all the possibly overlapping holes identified by VoidFinder. The merging of the holes forms each unique void region. This catalog is useful for identifying the entire void distribution of the Universe. All of the volume enclosed by these holes lies in void regions and all galaxies contained are considered void galaxies. The third catalog consists of the location and effective size of each unique void region. This catalog is useful for identifying overall void statistics in the Universe. Study of large scale structure as well as void volume distributions can be calculated from this catalog. Along with the three catalogs is the catalog of void galaxies. We have identified all galaxies with spectra that lie within the void regions identified by VoidFinder. These catalogs can be downloaded for use[1].

We have now identified the largest and most comprehensive void catalog from the largest spectroscopic data set available. Previous studies of voids from earlier data releases of SDSS, and other surveys including 2dF Galaxy Redshift Survey all lack the combination of completeness, depth, and contiguous sky provided in SDSS DR7. There is no longer an issue with survey boundaries restricting the volume of study for finding large voids. As there are currently no plans for a large spectroscopic survey of L* galaxies, this will be the most comprehensive data set for years to come.

2.7 Summary

We studied the distribution of cosmic voids and void galaxies using Sloan Digital Sky Survey data release 7 using an absolute magnitude cut of $M_r < -20.09$. Using the VoidFinder algorithm as described by Hoyle and Vogeley [2002], we identify 1054 statistically significant voids in the northern galactic hemisphere greater than 10 h^{-1} Mpc in radius, covering 62% of the volume. There are 8,046 galaxies brighter than $M_r = -20.09$ that lie within the voids, accounting for approximately 6% of the galaxies, and 79,947 void galaxies (11.3%) with $m_r < 17.6$. The largest void is just over 30 h^{-1} Mpc in effective radius. The median effective radius is 17 h^{-1} Mpc. Voids of size $r_{eff} \sim 20h^{-1}$ Mpc dominate the void volume. The voids are found to be significantly underdense, with $\delta < -0.85$

[1] www.physics.drexel.edu/∼pan/

near the edges of the voids. We tested the sensitivity of the void finding algorithm to changes in the absolute magnitude cut within the range $-19.6 > M_r > -20.6$. The resulting void regions are largely similar with slight differences only near the edges of the void regions. The radial density profiles of the voids are found to be similar to predictions of dynamically distinct underdensities in gravitational theory. We compared the results of VoidFinder on SDSS DR7 to mock catalogs generated from a SPH halo model simulation as well as other Λ-CDM simulations and found similar results, ruling out inconsistencies resulting from selection bias and survey geometry.

Chapter 3

Alternate Void Finders and Void Catalogs

3.1 Comparison to Watershed Void Finder

The void finding method used in the previous chapter is a purely galaxy based void finding algorithm. Colberg et al. [2008] discusses the many different void finders available, one in particular is the Watershed Void Finding method [Platen et al., 2008]. The Watershed Void Finder (WVF) uses Delaunay Tessellation Field Estimator [Schaap and van de Weygaert, 2000] to estimate a density field based on a magnitude limited sample of galaxies. WVF utilizes a sample of galaxies as tracers for dark matter haloes. By assuming that each galaxy lives in the center of a particular halo, one can construct a cosmic web of dark matter. Using the same data set, we can compare the results of the different void finders.

Figure 3.1 shows a redshift slice of the Universe that includes both the Watershed Void Finder and VoidFinder results. The figure was constructed to point at the nearby Bootes "supervoid", which can be seen on the left edge of the figure. As can be seen in both the DTFE smoothed field as well as VoidFinder, the Bootes "supervoid" is actually a concentration of a group of voids. They may some day merge, but currently there are still well defined galaxy filaments that separate individual smaller voids. The underlying density field is well traced by the VoidFinder galaxies and

the characteristic size of voids found with the Watershed Void Finder is similar.

3.1.1 Void Matching

Figure 3.2 shows the matching distance between voids found using the Watershed Void Finding method and VoidFinder. The majority of voids are found to match within the radii of each other, while a couple of voids are found to have matching distances right near one void radius. In the event that one void finding algorithm identifies two separate voids while the other combines the two into a single void, we expect an overmatching to occur right at the distance of one void radius and that is what we are seeing here. Figure 3.3 shows the matching fraction of voids as a function of the distance from the center of the VoidFinder void the corresponding match was found. The overall volume of voids is well matched compared to the WVF method ($\sim 85\%$).

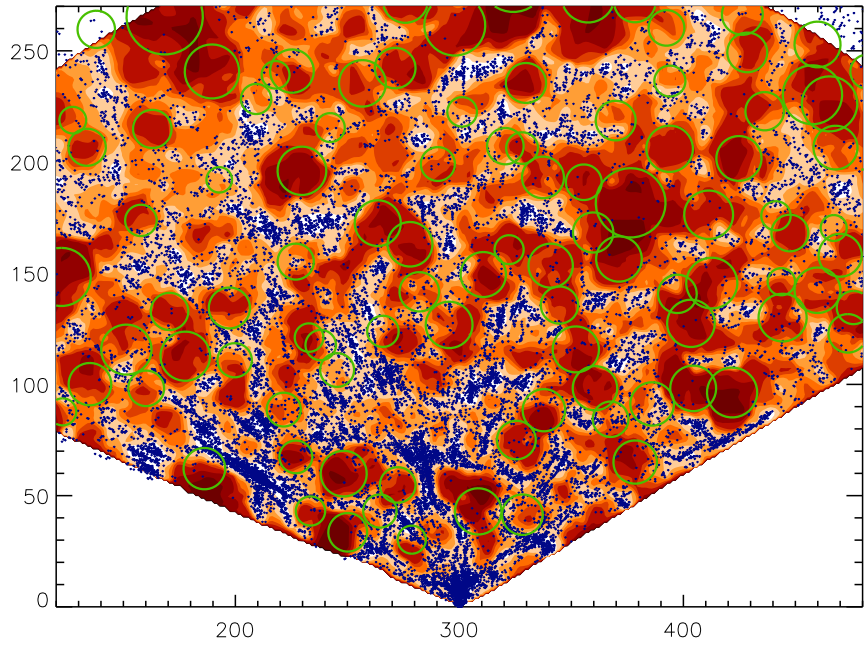

Figure 3.1: A 10 h^{-1} Mpc thick slice of the Universe that includes the center of the Bootes 'super'void. The void can be seen on the left edge of the figure as a group of smaller voids with thin filaments separating them. Both WVF and VoidFinder have identified this region is a group of smaller voids. VoidFinder does a good job of tracing out similar underdense regions as the Delaunay Tessellation Field Estimator.

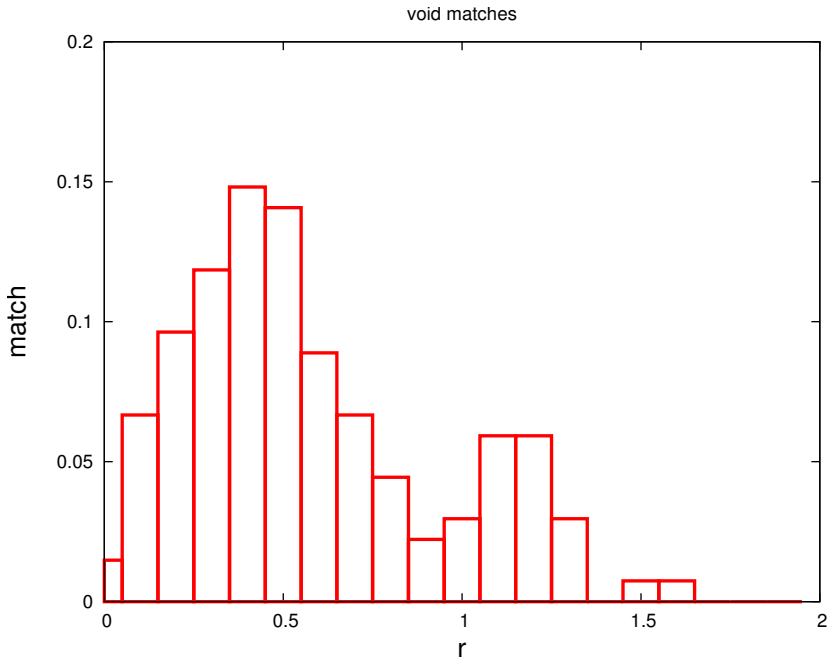

Figure 3.2: The distribution of void matches of large voids (radius $> 20\ h^{-1}$ Mpc) between the two algorithms, one found by VoidFinder, and the other identified by the density field show that a large fraction of voids are well matched in both algorithms. The x-axis is the distance r = r_{match}/r_{void} where r_{void} is the radius of the void as found by VoidFinder

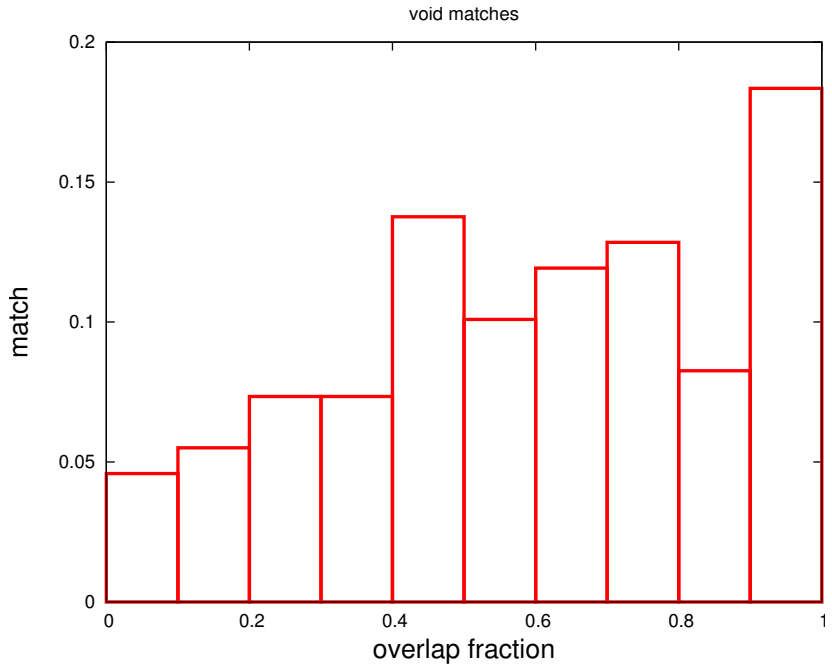

Figure 3.3: The overlap fraction of large voids (radius $> 20\ h^{-1}$ Mpc) identified using the two different algorithms. The overlap fraction is defined by $V_{overlap}/V_{VF}$ where V_{VF} is the volume of the void in VoidFinder

3.2 Other Void Catalogs

While the Sloan Digital Sky Survey focused its observations on the northern galactic hemisphere, a similar, but shallower, redshift survey was carried out in the southern galactic hemisphere. The 6dF redshift survey [] covers approximately 25,000 square degrees of the southern sky, obtaining spectra for 117,191 galaxies. A volume limited sample of galaxies was chosen with limiting z $<$ 0.05 and a similar absolute magnitude limit of M $<$ -20.1. This resulted in a volume limited sample of 21,641 galaxies. Figure 3.4 shows the sky coverage of 6dF. It covers much more of the sky than the SDSS, however, it suffers from a large swath of 'problem' areas with bad spectroscopy and lack of survey depth, making it a less ideal redshift survey for three dimensional void finding than the SDSS. In 6dF, we find 219 voids with r $>$ 10 h^{-1} Mpc, average r_{eff} = 17.86 h^{-1} Mpc, and 1,296 volume limited void galaxies.

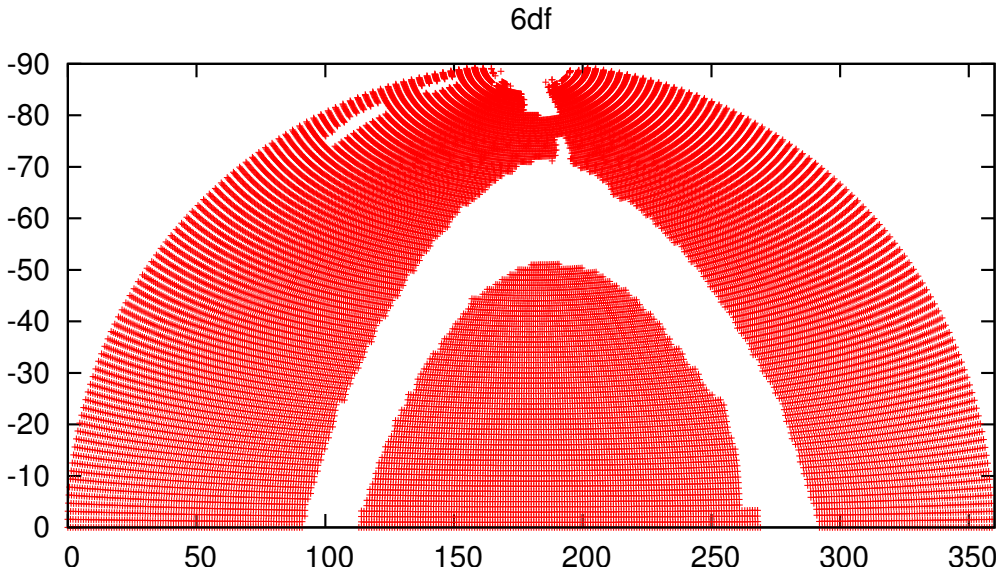

Figure 3.4: Southern sky coverage for 6dF. It covers almost the entirety of the southern sky, including some overlap area with the SDSS coverage of the northern galactic hemisphere.

3.2.1 Radial Density Profiles

Comparing the radial density profiles of voids from 6dF to those found in the SDSS (Figures 3.5 and 3.6), we see that the results are very similar. We do not expect there to be a difference in the density profiles of voids from the northern galactic hemisphere compared to the southern galactic

hemisphere.

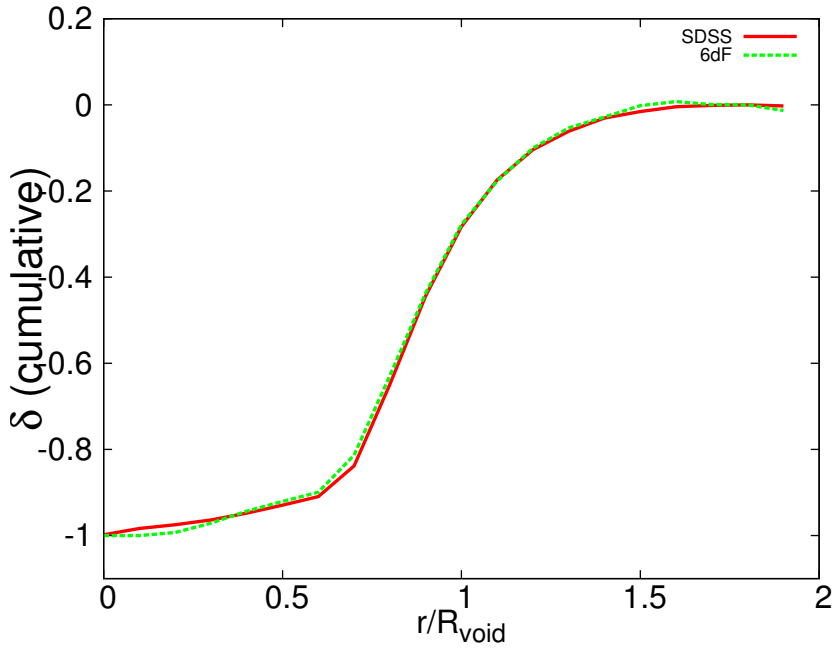

Figure 3.5: A comparison of the radial density profile as a function of effective radius. The cumulative density is calculated and compared, the two curves are nearly identical, showing that voids in the northern hemisphere are similar to their southern hemisphere counterparts.

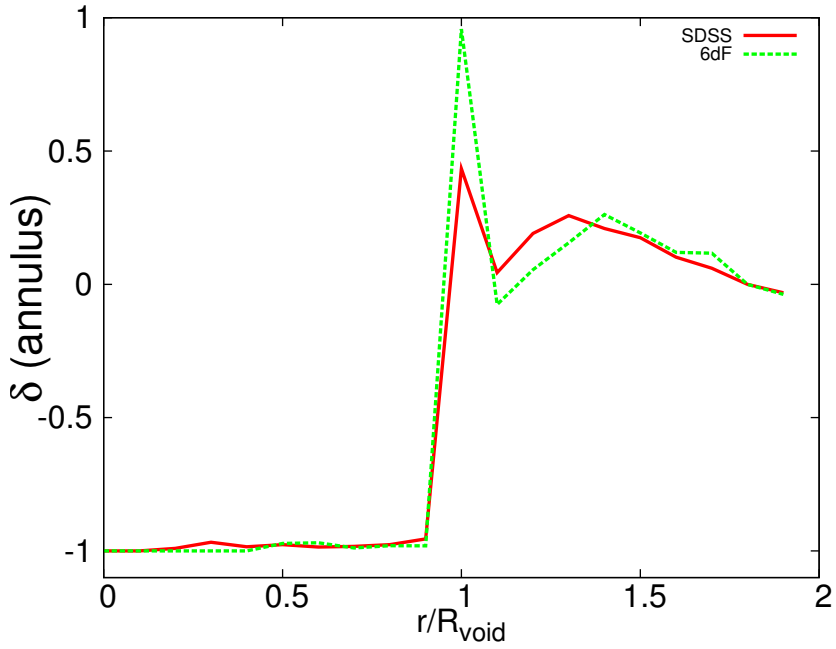

Figure 3.6: A comparison of the radial density profile as a function of the maximal void sphere radius. The density is calculated in a spherical annulus, and the major features (bucket shape) are once again very similar.

3.3 Alternate Cosmological Models

Void finding is also done to test the capabilities of other models of cosmology. It is important to consider other possible explanations to the modern day problem of cosmology and not become too focused on just one possible solution. While the standard model of cosmology (ΛCDM) is particularly attractive in matching all the statistics of the angular power spectrum of the Universe, supernovae, gravitational lensing, cosmic microwave background, and the velocity dispersions of the arms of spiral galaxies, it is not the only possible solution. There are a number of simulations done with variations on the supposed cosmological model. Some of these include non-linear models of gravity as well as non-Newtonian models of gravity. The preservation of large scale structure must remain when considering the results of these simulations. We have run VoidFinder on a number of these simulations and tested their ability to predict large scale structure in the Universe.

3.3.1 Non linear gravity models

There have been several groups that have investigated the effects on large scale structure of non-linear coupling of modes at large scales. Takahashi et al. [2008] use the cosmological simulation code GADGET-2 [Springel, 2005] to simulate the Universe in a volume with L = 500 h^{-1} Mpc and 256^3 particles. The initial conditions are calculated using results from the cosmic microwave background (WMAP). The initial conditions are assumed to be a Gaussian random field. For small scales, linear perturbation theory predicts structure fairly accurately. However, at large scales the second order perturbation predictions begin to deviate from the first order perturbation terms. Using results from WMAP and SDSS BAO, Takahashi et al. [2008] generated simulations to test the growth of large scale density fluctuations, and I have applied VoidFinder to these results. Figure 3.7 show the radius histograms of observed SDSS results compared to two different simulations. Figure 3.8 show the radial density profiles of observed SDSS results to the same two simulations. For both models, the size distribution of voids are similar to observed SDSS results, and the radial density profile shows the same bucket shaped result as well.

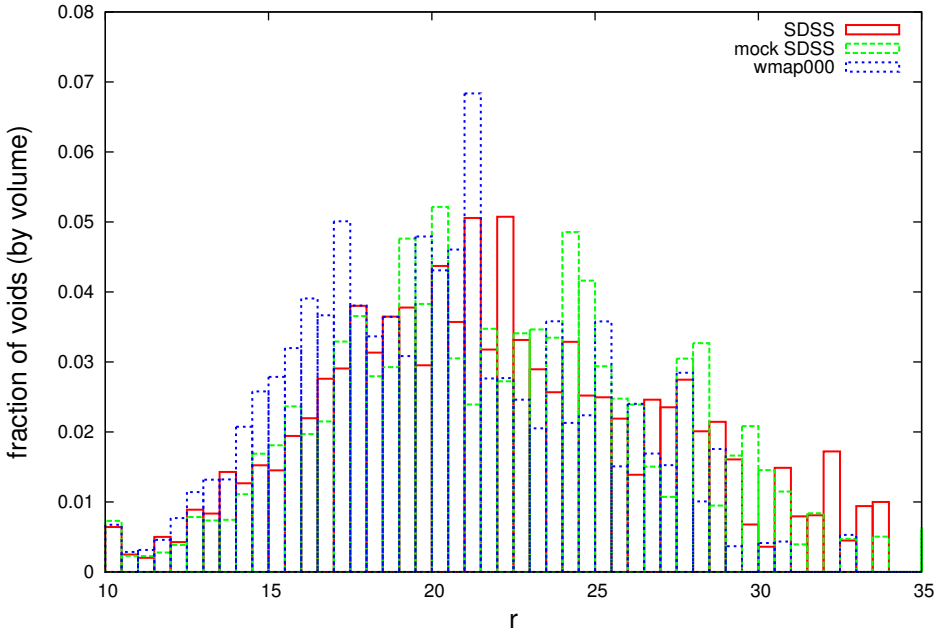

Figure 3.7: The radius histogram of voids found in a non linear model, standard model, and SDSS shows no major discrepancy in the typical sizes of large scale voids. While there may be differences in individual columns of the histogram, the overall shape of the distribution of void sizes is preserved.

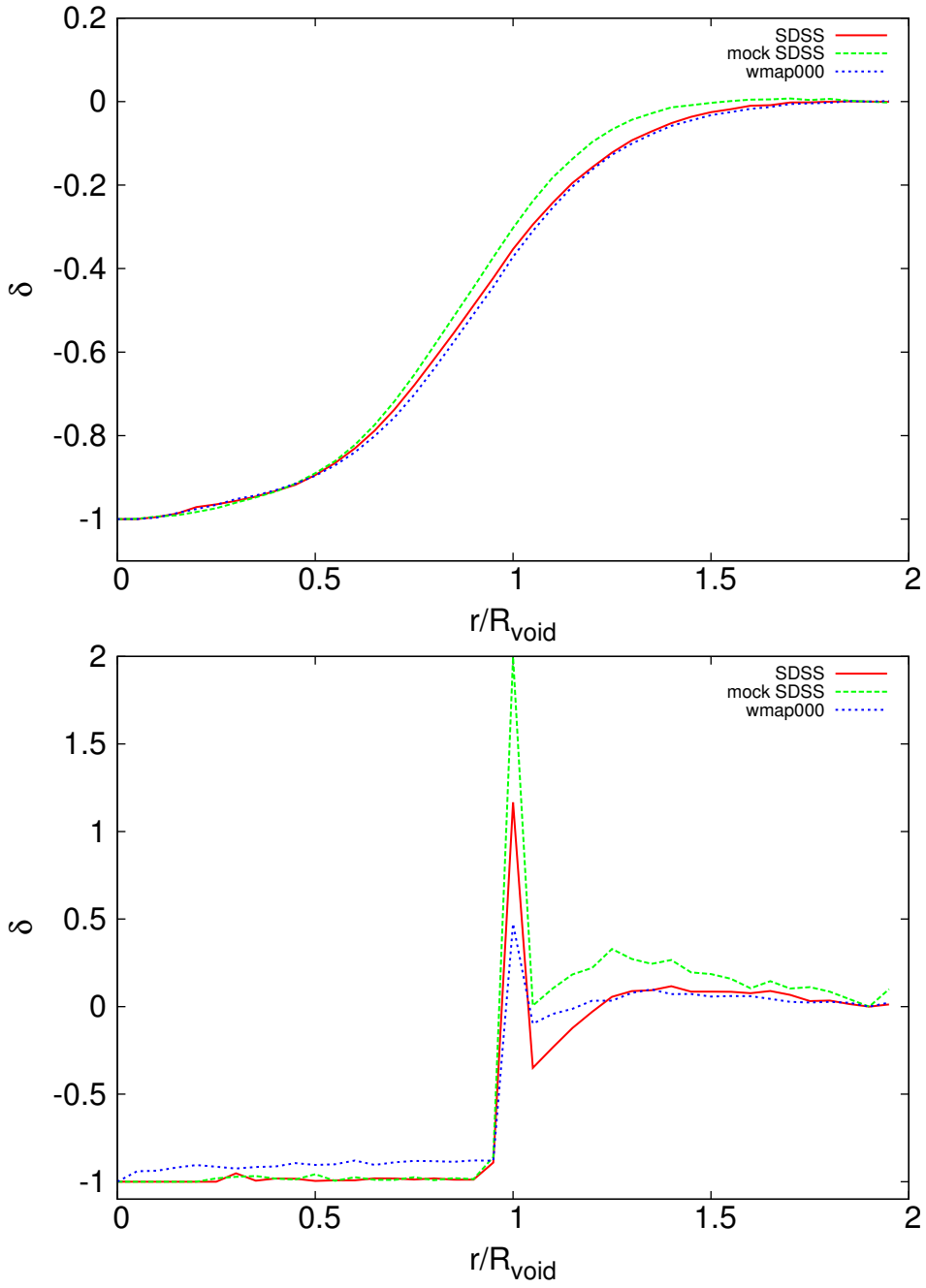

Figure 3.8: The average radial density profile of voids after scaling the profiles by R_{void} and stacking. The radial density profiles of voids found using nonlinear models and using the standard model of cosmology closely matches with the radial density profile of observed voids. Both types of simulations appear to accurately simulate the extreme underdensities in the centers of large scale voids, and a sharp overdense structure at the edges of voids.

Chapter 4

Void Shapes

Observed voids are expected to be spherical. Icke [1984] explains why voids should be spherical by comparing it to numerical simulations of pregalactic clouds. Numerical simulations done by Dekel [1983], Hoffman et al. [1983] show that gravitational collapse of matter tends to form filamentary structure. Density inhomogeneities collapse such that any asphericity is enhanced as the structure grows. Considering voids as massively underdense regions, it is possible to simply consider the local density inhomogeneity as having a negative density gradient compared to the overdense regions. The net effect is simply the inverse of a dense gravitational collapse, any asphericity will be pushed towards becoming more spherical, and the voids would grow in size. The size of the void is sensitive to cosmological parameters, particularly the amount of dark energy present in the Universe and the value of σ_8 the average density of matter in a randomly placed sphere of 8 h^{-1} Mpc. Shandarin [1994] looks at the size of large scale structure in the Universe under the conditions of nonlinear dynamics. He finds that large scale structure tends to specific sizes given what Ω_0 is assumed to be. In the dark energy dominated era, local void sizes are most sensitive to the amount of dark energy, Ω_Λ. Later on, Shandarin et al. [2006] find underdense regions in a series of cosmological simulations. They compare various values of σ_8 to the volume filling factor of voids and tests the robustness of void finding in the simulations. They find that even in simulations, voids can appear aspherical and are slightly sensitive to varying values of σ_8. It is important to gain a better understanding of what

the sizes and shapes of voids are to better understand how large scale structure is distributed in our observed Universe in order to compare to cosmological models.

4.1 Void Regions: Spherical?

In the work described in chapter 2, a void catalog was created that described void regions with both a maximal sphere and an effective radius. The maximal sphere described the largest empty sphere that filled the void region, whereas the effective radius describes the overall volume of the void. While void regions are expected to be generally spherical in nature, there are many things that can cause void regions to remain aspherical. Effects such as redshift space distortions, dark energy, and Universe inhomogeneity can all play a role in defining the overall shapes of large scale structure.

4.2 Redshift Space Distortions

Observational cosmology is based on determining the distance of objects based on its redshift. The distance to an observed object is defined by an expected shift of observational lines in the spectrum of an object due primarily to the expansion of space as the light from the object traveled to the observer. If we consider observing absorption lines in the spectrum from a galaxy, we know the approximate shape of the spectrum at various wavelengths given the luminosity of the galaxy, and we expect that at specific wavelengths there could be absorption due to gas in the galaxy. These absorptions occur at these specific wavelengths in the rest frame of the galaxy. However, due to the expansion of space, as light from the galaxy travels to the observer, the light becomes redshifted. Alternatively, if space were shrinking, we would expect the light to become blueshifted. The effect on the observed lines can be seen in Figure 4.1.

Complicating the matter of determining distance using redshift, however, is the degeneracy in observation of objects that are physically moving either towards or away from the observer. The result of this effect is known as redshift space distortion. Observers see the Universe in redshift space, and not real space. Since galaxies can have peculiar motions, measuring the redshift to a galaxy does not give us the distance to the galaxy, the redshift observed is a combination of the distance to the galaxy and its local peculiar motion in space. Distortion effects such as the finger

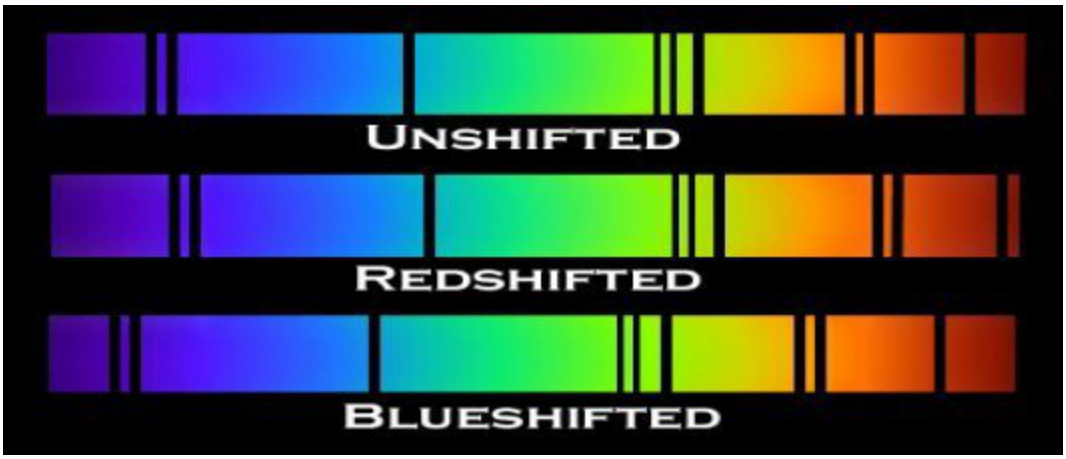

Figure 4.1: Unshifted, redshifted, and blueshifted spectral absorption lines are shown. A galaxy that is moving away from us due to the expansion of space will have its lines redshifted. A blueshift occurs if a galaxy was found to be moving towards us.

of god effect and systematic infall can cause observational errors when determining the distance to galaxies.

4.2.1 Finger of God effect

The finger of god effect occurs when a distribution of galaxies is collapsing into its center. A group of galaxies that may have a spherical spatial distribution is seen in redshift space having redshifts that are caused both by the real distance to the galaxy and their local velocity. A large cluster of galaxies can lead to large peculiar velocities that can cause a large error in measuring the distance to the galaxy. The resulting distribution is a oblong ellipsoid stretched out along the line of sight to the galaxy cluster. This is known as the finger of god effect and it can be seen clearly in the famous CFA stickman figure from de Lapparent et al. [1986], seen below in Figure 4.3.

4.2.2 Systematic Infall effect

Systematic infall occurs when galaxies in the linear regime (large scale voids) are drawn to gravitational sources (large scale filaments). The overall effect of systematic infall can be seen in the top row of Figure 4.2. As galaxies are ejected by the voids (gravitationally attracted to the filamentary walls of the voids), we can observe the voids to take a shape that is "squashed" in redshift space.

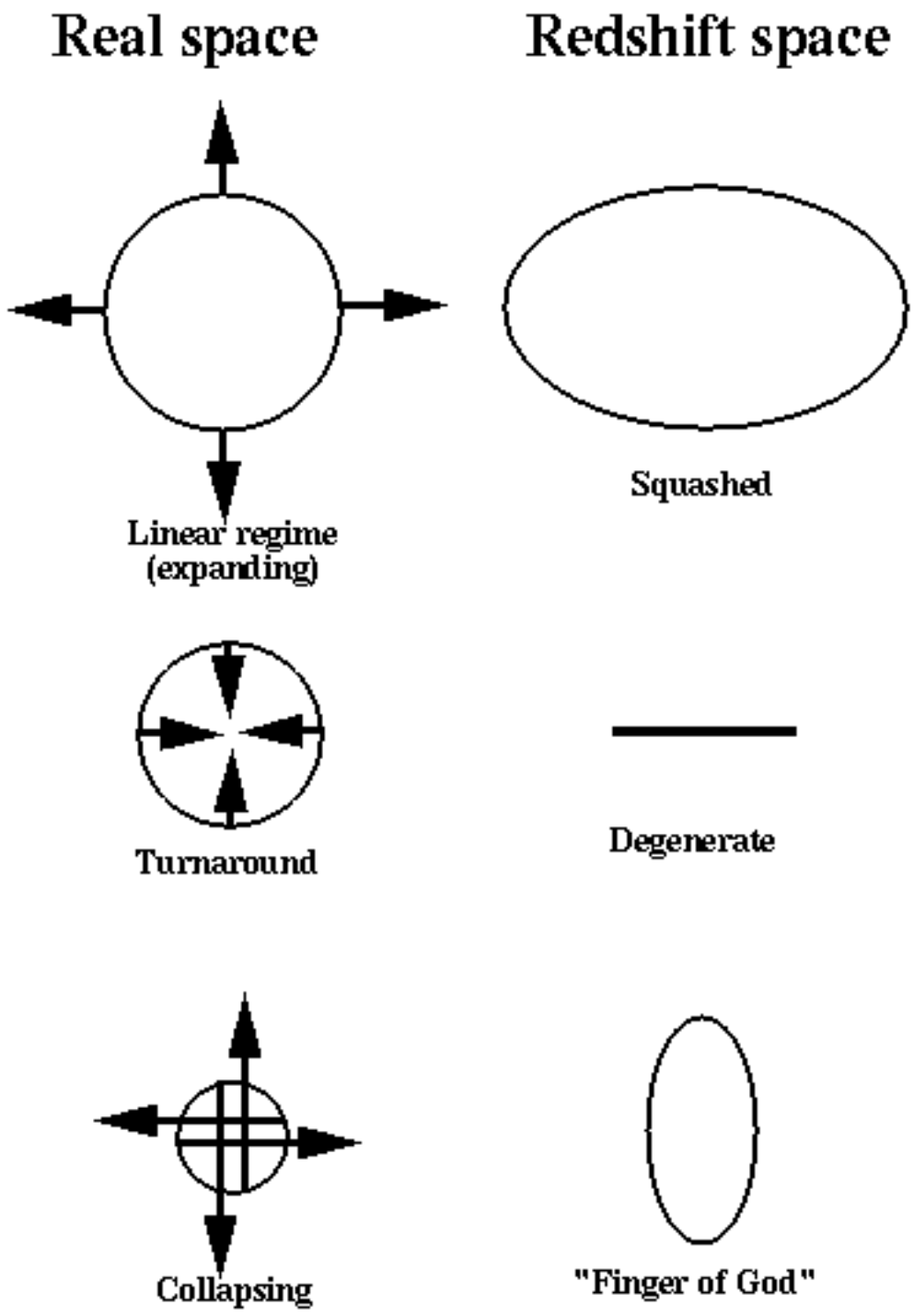

Figure 4.2: The results of different types of galaxy distributions can be seen in this figure in both real and redshift space. The top row shows that a linearly expanding spherical distribution of galaxies will be seen as a squashed distribution in redshift space. The bottom row shows that a collapsing spherical galaxy distribution can lead to the finger of god effect.

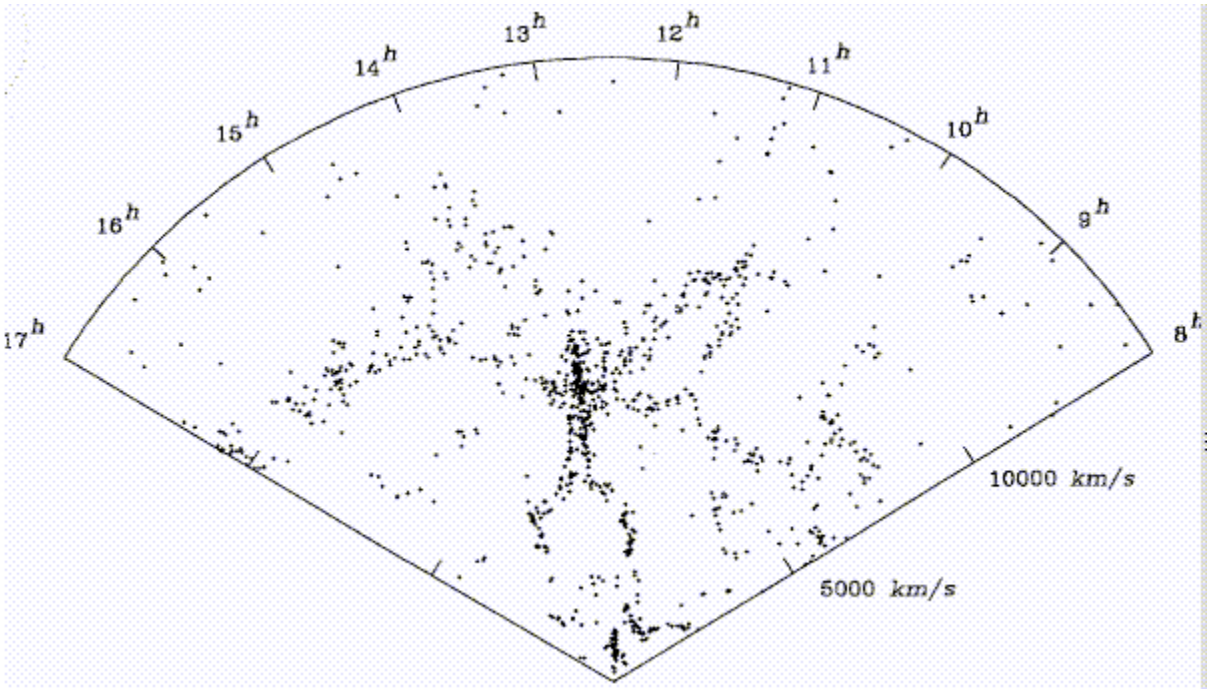

Figure 4.3: Slice of an early redshift survey [de Lapparent et al., 1986] that clearly shows the finger of god effect. A local nearby cluster of galaxies can be seen stretched into a long cylindrical shape, and the large distribution of galaxies in the center of the slice has been stretched as well.

4.2.3 Redshift Distortion Effects on Void Properties

The two competing effects of redshift space distortions act opposite to one another in the observation of the shape of voids. Fingers of god will cause a void to become more elliptical with the major axis pointing along the line of sight, and systematic infall will cause a void to become more elliptical with the major axis anti-aligned to the line of sight. Ryden and Melott [1996] found that the mean void size and maximum void size both increase going from real space to redshift space. The principal axes of the largest voids increased in size in redshift space, and tended to increase the size of the void along the line of sight, meaning finger of god effects dominated.

4.3 Mock Data

To determine the effects of redshift space distortions, it is important to be able to differentiate between results that may be seen in real space versus that of redshift space. Since it is impossible for observations of real space to be made, we have to rely on cosmological simulations to provide

us with insight into the behavior of galaxies as observed in redshift space. The mock catalog used is a dark matter only model [Skibba and Sheth, 2009] enclosed in a cube with sides 480 h^{-1} Mpc. The luminosity function and luminosity weighted correlation functions of the mock catalogue are fit to SDSS as described by Skibba et al. [2006], using halo occupation constraints from Zheng and Weinberg [2007]. The simulation parameters, in particular Ω_M and σ_8 are given in Yoshida et al. [2001]. The mock catalog used contains both real space coordinates as well as redshift space coordinates given with a modified z-axis. The observer is assumed to be at a location distant along the z-axis, allowing the axis to be used as a line of sight. In the simulation, the three dimensional velocities of the individual galaxies are known, and redshift space distortions can be included.

4.4 Fitting Ellipses

The first order correction to the shapes of voids is to consider regions to be triaxial ellipsoids. We fit best fit ellipsoids to void regions found in the previous chapter using the method described by Jang-Condell and Hernquist [2001], Shandarin et al. [2006], Foster and Nelson [2009]. We assume that void regions are empty and are described as a single large underdense object. This means that each section of volume in the entire void region is similar and is not given extra weight based on its local density. From the center of each void region, we define the shape tensor as follows.

$$S_{ij} = -\sum(x_i * x_j) \tag{4.1}$$

$$S_{ii} = \sum(x_j^2 + x_k^2) \tag{4.2}$$

The eigenvalues of the shape tensor then describe the three axes of the best fit ellipsoid as follows.

$$a_i = 5/(2N)[e_j + e_k - e_i] \tag{4.3}$$

$$a_j = 5/(2N)[e_i + e_k - e_j] \tag{4.4}$$

$$a_k = 5/(2N)[e_i + e_j - e_k] \tag{4.5}$$

The eigenvectors of the shape tensor describe the spatial direction of the axes of the best fit ellipsoid.

4.5 Results on Void Shapes

Figure 4.4 shows a slice of SDSS with the comparison of a best fit ellipsoid plotted against the maximal sphere of the void region. The best fit ellipsoid appears to fill in the void volume much better than the maximal sphere, it also preserves the volume of the void region. The results of void ellipticity in the void catalog can be seen in Figure 4.5. The three axes of the ellipsoid, $a \geq b \geq c$, can be described by the two ratios b/a and c/b. We can see that there appears to be a slight preference for the ellipsoidal void regions to have a prolate shape as opposed to an oblate shape. Prolateness can be seen in the figure as an excess of points with smaller b/a compared to c/b, an example of an object that is prolate is an American football, or a rugby ball. Oblateness is seen as an excess of points with smaller c/b compared to b/a, and example of an object that is oblate is a pancake, or a disk. A similar result can be seen (Figure 4.6) when looking at voids in real versus redshift space using the mock simulations described in a previous section. This means that the excess prolateness is not caused by redshift space distortions. It is likely due to a preference for voids to merge in pairs for the resulting observed void to be a prolate ellipsoid. More analysis into the substructure of voids needs to be done to confirm this assessment. As a whole, voids are generally spherical in shape, with no major deviation for being highly elliptical. This is expected as we expect large scale voids to become more spherical over time. Similar results can be seen in void shape analysis done by Foster and Nelson [2009] on a subsample of voids from SDSS DR5.

To determine the cause of asphericity in voids, we calculate void shapes on a set of mock simulations. These mock simulations exist for both redshift and real space, allowing us to see the difference in shape finding on redshift space distortion effects. By measuring the alignment along the line of sight of the principal axis of the void region (Figure 4.8 and 4.9), we see that there appears to be no preference for redshift space distortions in determining the shape of the voids. This means that the finger of god effect and systematic infall are not playing a large role in defining the actual shapes of the voids. However, looking at the radius histogram of void sizes, redshift space distortions will

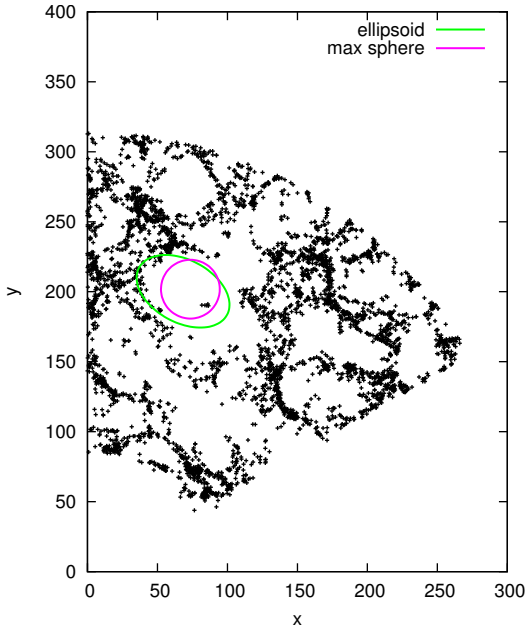

Figure 4.4: Example of a best fit ellipsoid fit compared to the maximal sphere of the void region. The best fit ellipsoid does a much better job of describing the void region and filling in the void volume than the maximal sphere.

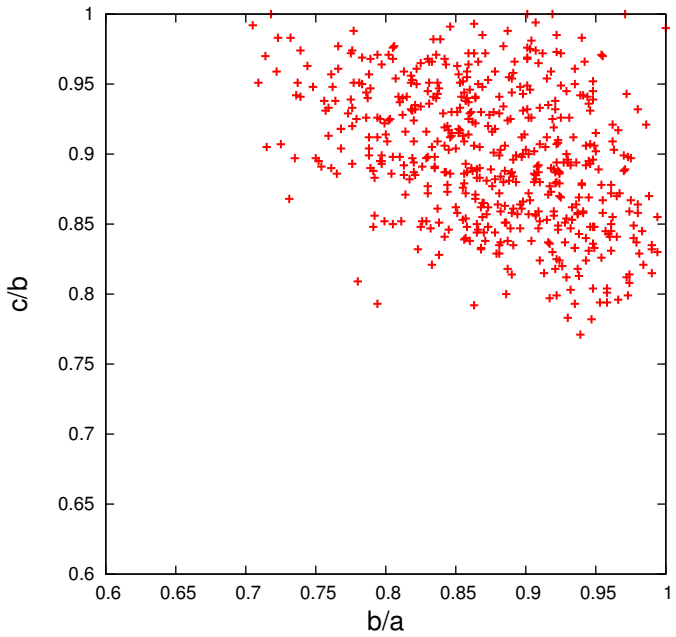

Figure 4.5: A comparison of the axes of the best fit ellipsoid. Most of the voids are spherical in shape, however, there is a slight preference for voids to be prolate rather than oblate if it is aspherical.

effectively enlarge individual void regions for large voids as seen in Figure 4.7, but the effect is less pronounced for smaller voids.

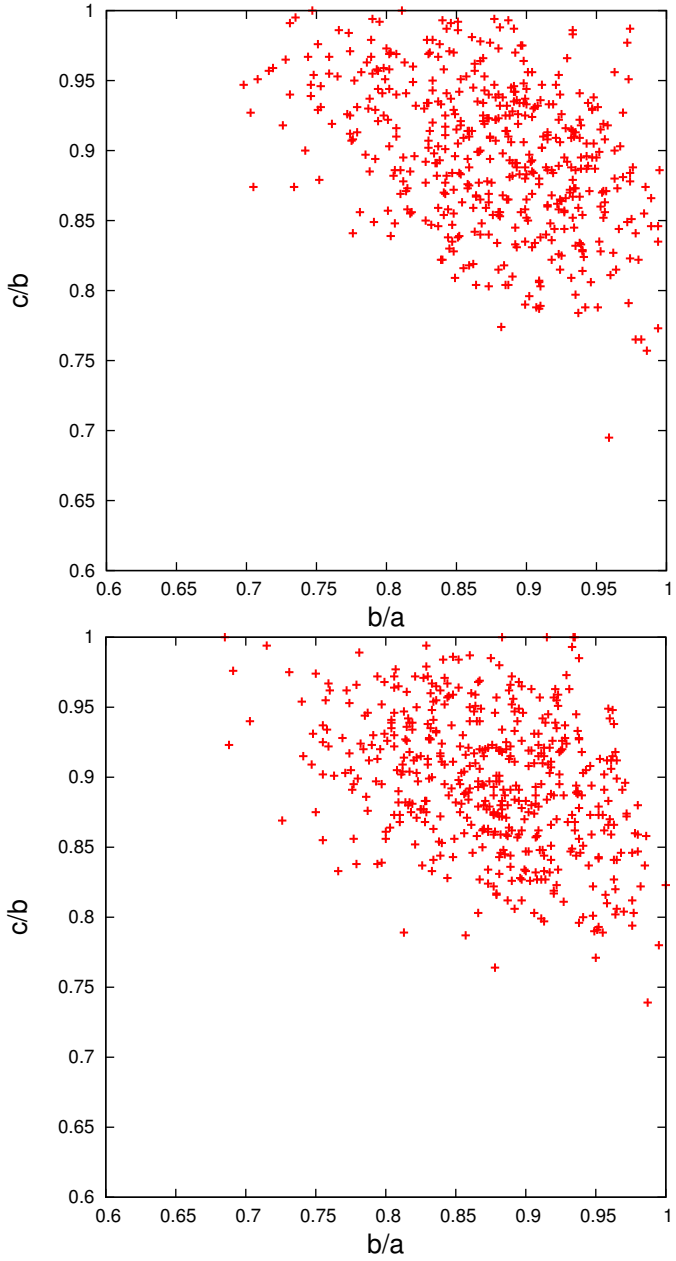

Figure 4.6: Comparison of axes of the best fit ellipsoid for simulated mock samples in real(left) and redshift(right) space. The distribution of ellipticity appears nearly identical, the preference for prolateness is still apparent.

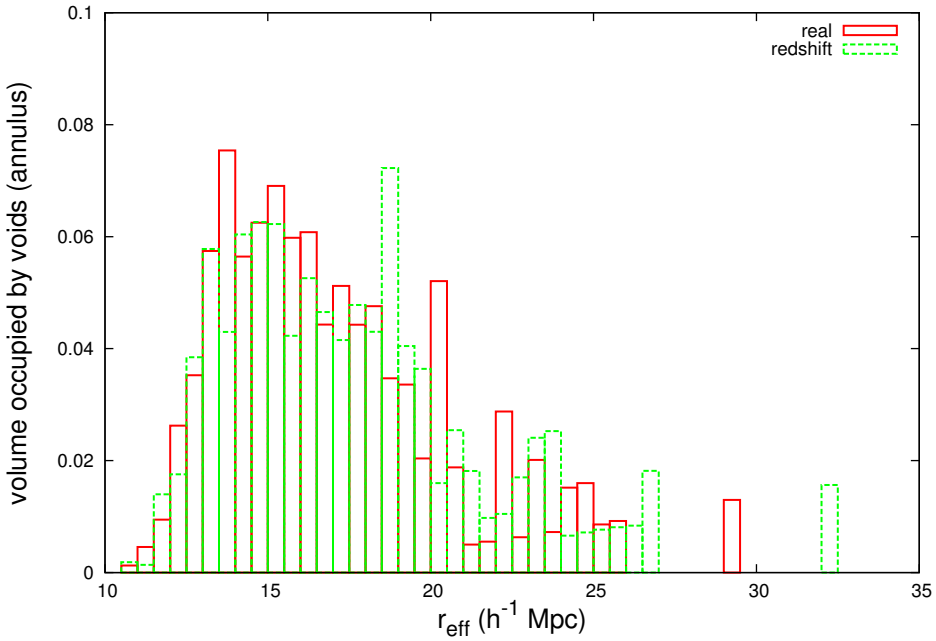

Figure 4.7: Radius histogram for voids found in real space and redshift space using a mock simulation. Void sizes are largely similar for both samples except for larger voids. There is a tendency for large voids to appear much larger due to redshift space distortions.

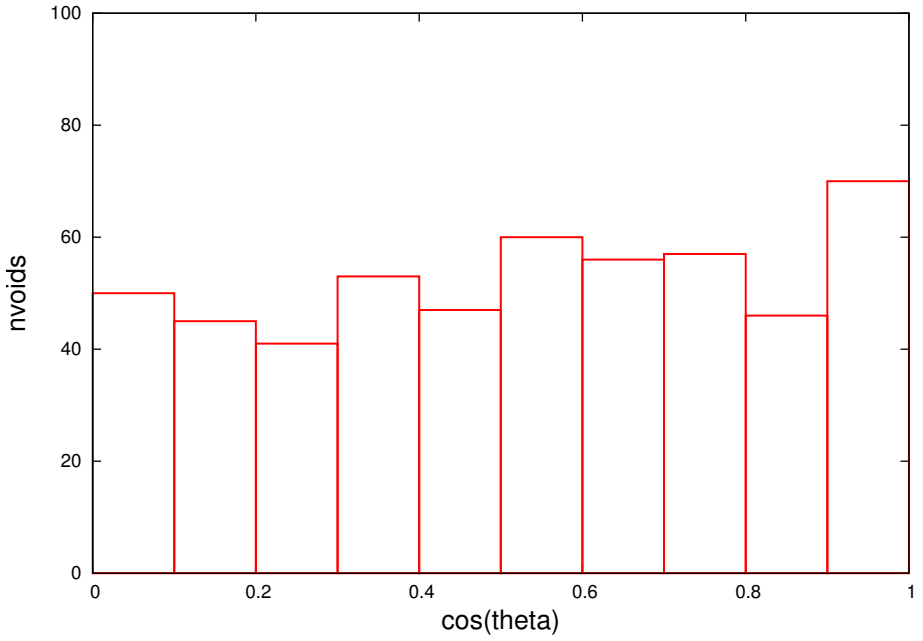

Figure 4.8: The line of sight alignment histogram shows minor variations from bin to bin, there does not appear to be any preferred direction for the major axis of the best fit ellipsoid to the line of sight.

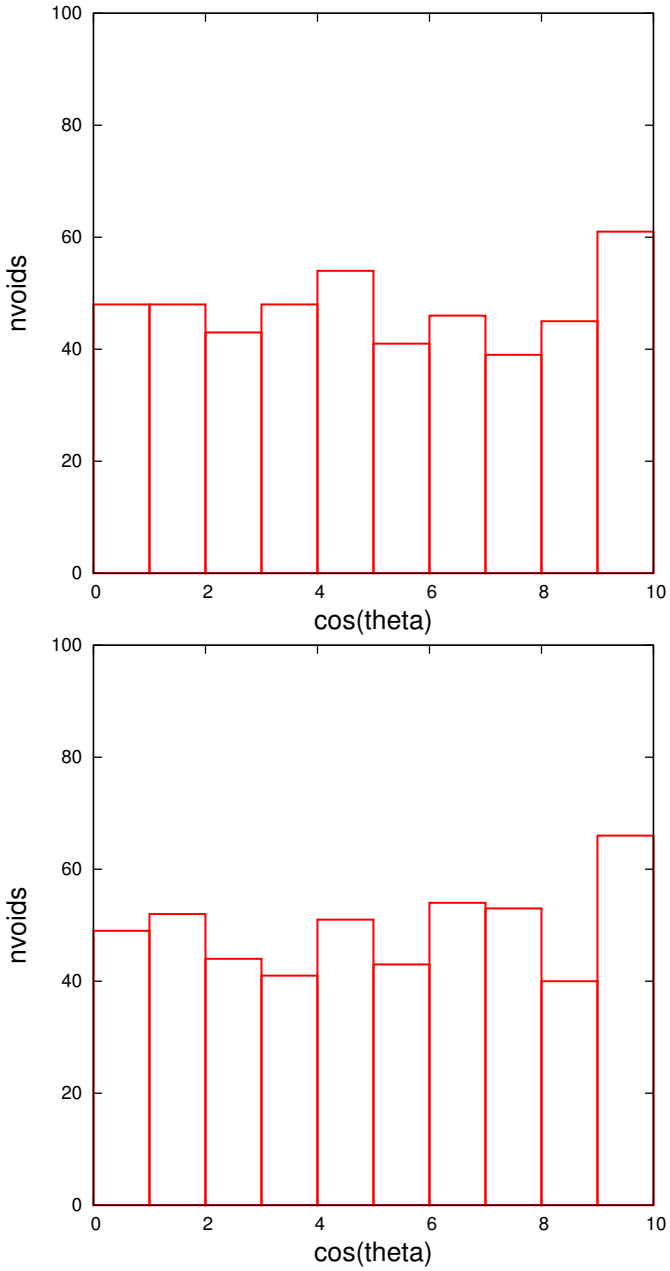

Figure 4.9: A comparison of the line of sight alignment histogram in real(left) and redshift(right) space. Once again, there does not appear to be any preferred direction for the major axis of the best fit ellipsoid to the line of sight in either sample.

Chapter 5

Void Galaxy Distribution

The distribution of galaxies in the Universe can provide us with an understanding of the underlying cosmology that placed those galaxies in their locations today. As discussed in chapter 1, independent measurements of supernovae, BAOs, and CMB places constraints on the fundamental cosmological parameters that determine the standard model of cosmology, ΛCDM. The best estimates for cosmological parameters from SDSS BAO measurements by Percival et al. [2010] are $\Omega_m = 0.286 \pm 0.018$, and $H_0 = 68.2 \pm 2.2$ km s^{-1} Mpc^{-1}. Their results indicates $w \approx$ -1, showing a constant dark energy equation of state, and rules out curvature of space, $\Omega_k \approx 0$. These results match WMAP CMB measurements listed in 1.1.

These fundamental cosmological parameters determine the distribution of galaxies in the Universe and are the input parameters to cosmological simulations. The standard model of cosmology predicts precise distributions for the galaxies in the Universe. These predictions must match our observations, so we compare the small scale structure predictions of simulations to our observed Universe.

5.1 Two point correlation function

The two point correlation function of galaxies describes the clustering hierarchy of galaxies. If galaxies were spatially uncorrelated, the correlation function would be flat. However, a simple look at galaxy maps of the Universe tells us that galaxies are not uncorrelated, and at the very least

gravity plays a large role in the distribution of galaxies in the Universe. It is only recently that there have been sufficiently deep redshift surveys that probe the three dimensional structure of the Universe. The SDSS DR7 sample is the largest survey to date and provides an excellent three dimensional data set for calculating the clustering hierarchy of galaxies.

5.2 Method

To calculate the two point correlation function, we start with the probability that a galaxy is found centered on a randomly placed volume element dV.

$$dP = ndV \tag{5.1}$$

The joint probability that we find two galaxies centered inside two volume elements dV_1 and dV_2 with separation s is then proportional to the sizes of the volume elements.

$$dP = n^2[1 + \xi(s/s_0)]dV_1dV_2 \tag{5.2}$$

$\xi(s/s_0)$ then represents the reduced two point correlation function for the distribution. This function has been fit as a power law with the form

$$\xi = (s/s_0)^{-\gamma} \tag{5.3}$$

where $s_0 = 7.62 \pm 0.67\ h^{-1}$ Mpc and $\gamma = 1.69 \pm 0.1$ [Constantin and Vogeley, 2006].

This analysis is done using two different types of two point correlation functions, the Davis-Peebles estimator [Davis and Peebles, 1983], and the Landy-Szalay estimator [Landy and Szalay, 1993].

5.3 David-Peebles Estimator

The Davis-Peebles Estimator is defined as follows,

$$\xi(s) = (N_R/N_G) * (DD/DR) - 1 \tag{5.4}$$

where N_R is the number of random galaxies generated to fit the sample volume, N_G is the number of galaxies in the sample, DD is the number of data-data pairs at a distance s, and DR is the number of data-random pairs at the same distance. An advantage of using this estimator is that the selection function of the sky distribution of the sample of galaxies does not need to be known. A disadvantage of this estimator is that it has large variance and is inaccurate at large scales (s ¿ 100 h^{-1} Mpc).

5.4 Landy-Szalay Estimator

The Landy-Szalay Estimator requires knowledge of the sampling geometry, but it is supposed to provide a better result for the variance than the Davis-Peebles Estimator. It is defined as follows,

$$\xi(s) = (DD - 2DR + RR)/RR. \tag{5.5}$$

The disadvantage of using the Landy-Szalay Estimator is that because random-random pairs have to be calculated, the computation time for calculating the two point correlation increases dramatically over typical estimators that might rely only on data-random pairs. To gain the full advantage of the LS estimator, it is necessary to have approximately ten times more random points than data points.

5.5 Results of two point correlation function

We find that the results of the two different types of estimators used in the analysis are identical. This is due to the fact that the number of galaxy pairs exceeds the threshold under which the Landy-Szalay estimator would prove advantageous. We find that the void galaxies are less clustered than their wall counterparts, with $s_0 = 7.8$ and $\gamma = 1.2$. This is similar in comparison to work done by Abbas and Sheth [2006] which compared galaxies living in low density regions ($< 33\%$ mean density) versus their wall counterparts. It can be seen comparing Figure 5.1 and 5.2 that void galaxies are found to be less clustered than wall galaxies.

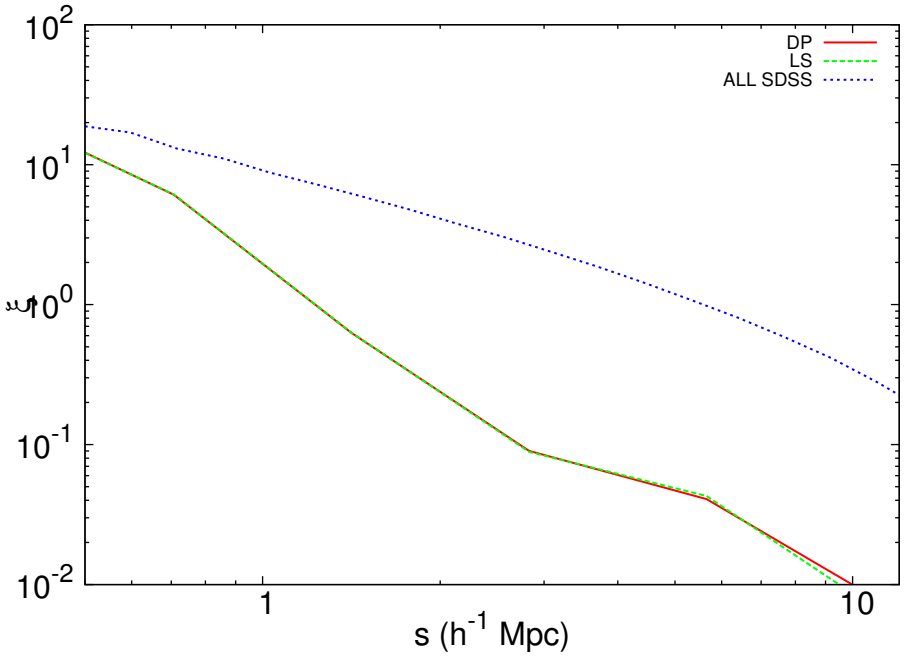

Figure 5.1: 2 point correlation function for void galaxies in SDSS. Values found using the Davis-Peebles estimator are identical to those found with Landy-Szalay. Compared to Figure 5.2 by Abbas and Sheth [2006], we also find that void galaxies are less clustered than its wall counterparts. Void galaxies are consistently less clustered than wall galaxies, and show a slightly steeper slope in the 2 point correlation function.

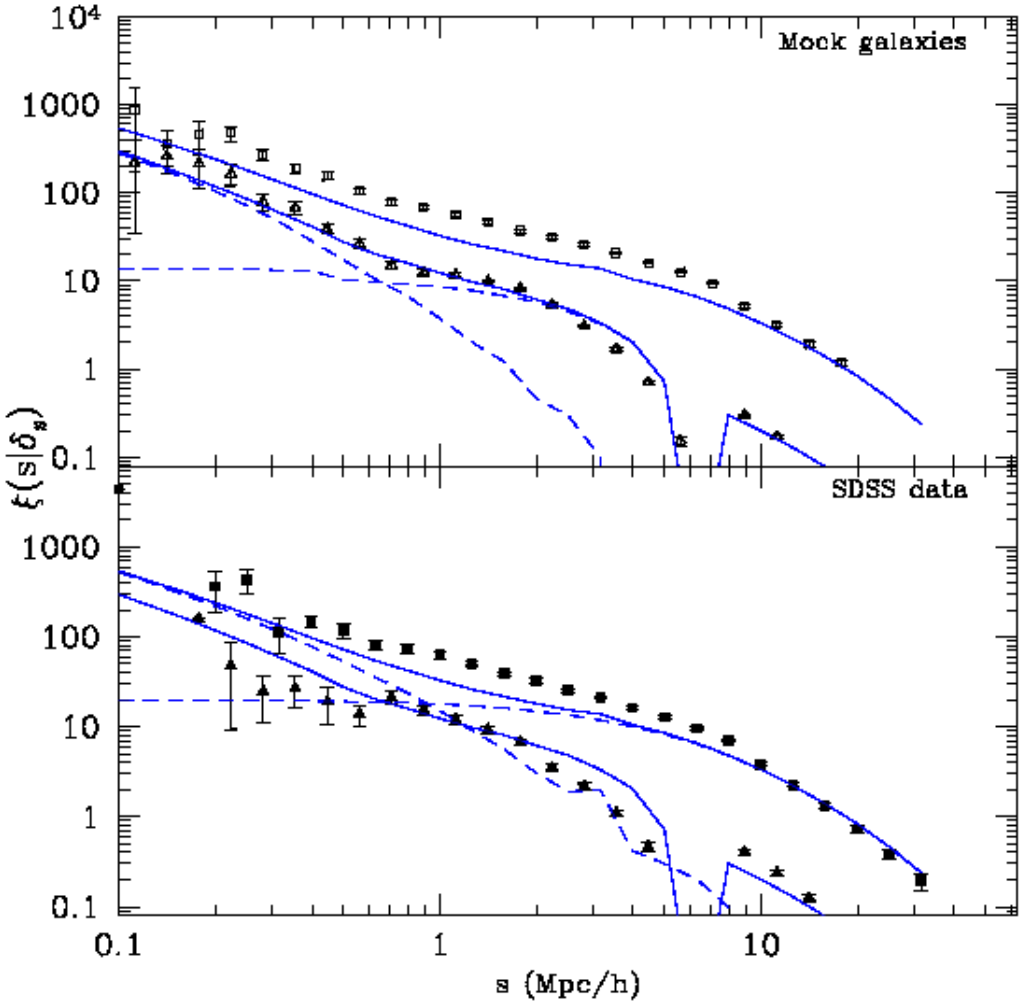

Figure 5.2: Plot from Abbas and Sheth [2006] that shows the 2 point correlation function for galaxies in SDSS and in mock SDSS samples. The curves are from the mock samples and the individual points are calculated from SDSS. The lower curve is found using galaxies that reside in low density regions using 8 h^{-1} Mpc spheres as the basis for determining the local density. The feature around 8 h^{-1} Mpc is probably due to the selection function for low density galaxies in the sample. The upper curve shows the 2 point correlation function for typical wall galaxies.

Chapter 6

Lyα Absorbers

Previous chapters have primarily focused on the distribution of voids and void properties, including the small scale structure of galaxies in voids. Now that we have a catalog of the locations of voids in the Universe, we can begin to look at the correlation of objects in the Universe to voids. The easiest things to look at are objects that are directly observable by telescopes. Baryons are the most easily detected objects in the Universe. In this chapter, we look at the distribution of baryons within voids, primarily looking at the local Lyα clouds.

6.1 Where are the Baryons?

Spergel et al. [2007] found that the cosmological density of baryons should be $\Omega_b h_{70}^2 = 0.0455 \pm 0.0015$. At high redshifts (z > 3), most of the baryons in the Universe are accounted for [Cen and Ostriker, 1999, Madau et al., 1998, Rauch et al., 1999, Weinberg et al., 1997]. However, at low redshifts, the distribution of baryons is largely unknown [Fukugita et al., 1996]; after including all observable forms of baryons, we are well short of the expected number observed at high z. This was described by Persic and Salucci [1992], Bristow and Phillipps [1994], Fukugita et al. [1998], Fukugita and Peebles [2004] as the "Missing Baryons Problem". Through numerical simulations [Cen and Ostriker, 2006, Davé et al., 2001, Smith et al., 2010], 40-50% of the baryons in the recent epoch should be found in the warm-hot intergalactic medium (WHIM). This gas is usually seen in the

UV traced by OVI [Danforth and Shull, 2008] and resides primarily in the intergalactic medium (IGM). After accounting for stellar mass in large local redshift surveys, the IGM must then contain approximately half of the baryons. Lyα absorbers are used for the identification of local IGM.

6.2 What are Lyα Absorbers

Lyα absorption is the absorption of photons by neutral hydrogen along the line of sight. This is typically observed by taking spectra of distant quasars [Hu et al., 1995, Lu et al., 1996, Kim et al., 1997, Burles and Tytler, 1997, McLin et al., 2002, Danforth and Shull, 2008]. As light travels from the distant quasar to us, neutral hydrogen along the way will absorb the light at the rest frame wavelength, thus, hydrogen clouds at different distances will absorb at a slightly different wavelength due to the expansion of the Universe.

Figure 6.1 shows spectra for both a nearby quasar and a distant quasar. The features of absorption by neutral hydrogen clouds can be seen as the Lyα forest [Lynds, 1971]. The more distant quasar (top) shows a much denser forest than the nearby quasar (bottom) because there are far more absorption clouds along the line of sight. The stronger the absorption feature, the larger the neutral hydrogen cloud that is doing the absorbing. Using absorption features to determine the locations of neutral hydrogen is incredibly powerful because it relies only on the strength of the background quasar and the column density of gas in the absorber. Detection of hydrogen clouds that emit very dimly in the optical is possible because all clouds with similar column densities along the line of sight can be equally detected. There is no bias towards more nearby hydrogen clouds because they may appear brighter due to proximity.

6.3 Previous Studies of Absorber Properties

Previous studies by Penton et al. 2004, Penton et al. 2002, Penton et al. 2000a/b have shown that the local Lyα absorbers are associated with the large scale structure of galaxies. In three separate papers, Danforth and Shull [2005], Danforth et al. [2006], Danforth and Shull [2008] studied the low-z IGM and determined the properties of Lyα absorbers and their metallicity contents with regards to their local environment. Furthermore, simulations by Cen and Ostriker [1999], Davé et al. [2001],

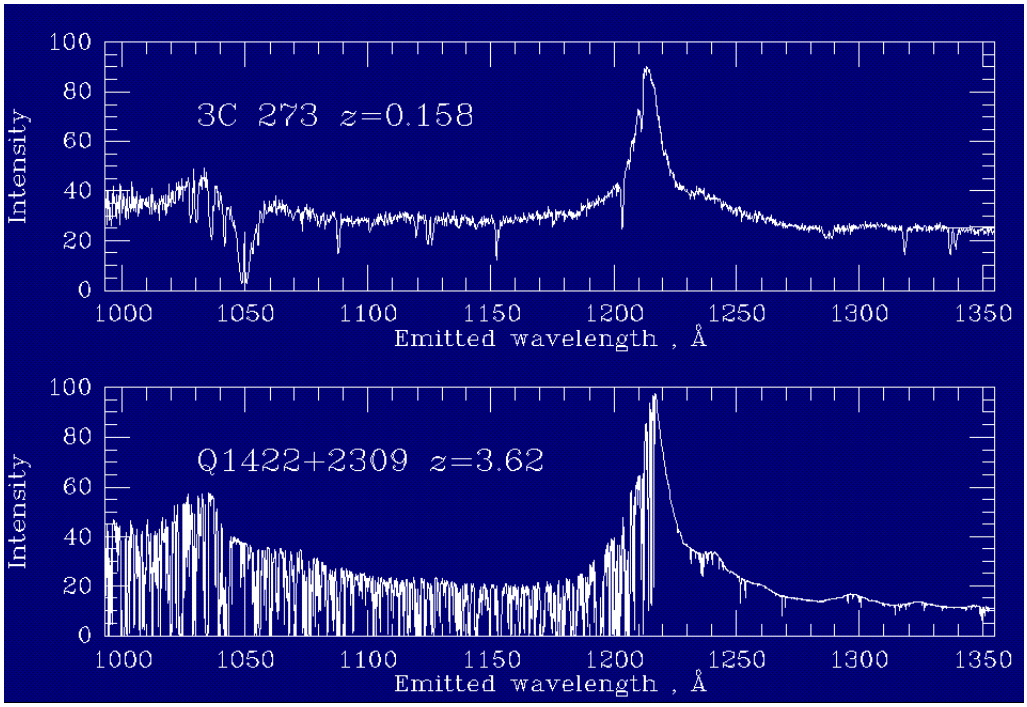

Figure 6.1: Quasar spectrum for 3C 273 (top, nearby) and Q1422+2309 (bottom, distant) show Lyα absorption. The distant quasar shows a much more prominent Lyα forest because there are far more neutral hydrogen clouds along the line of sight, primarily due to the distance between the quasar and the observer.

Smith et al. [2010] all assert that Lyα absorber observations are from partially photoionized clouds with shock-heated gas, showing features of sharp Lyα lines and OVI tracers of WHIM. It is generally assumed, then, that the Lyα absorbers are all found in the filamentary large scale structure of the Universe.

6.4 Where are the Absorbers?

McLin et al. 2002 and Penton et al. 2002 conducted a study on Lyα absorbers in galaxy voids that found a significant portion ($\sim$ 30%) of absorbers reside at least 2 h^{-1} Mpc from the nearest $M_b \leq$ -17.5 galaxy. Using HST observations of Lyα absorbers and deep pointed observations along the line of sight using HYDRA on WIYN, they predict that the total baryonic density in these 'voids' is 4.5% $\pm$ 1.5% of the mean baryon density assuming photoionization models for the clouds. Grogin and Geller 1998 found that Lyα absorbers appear more frequently in underdense regions than dense regions when compared to the number of galaxies in the regions. Using a sample of 18 local Lyα

Table 6.1: Names and Locations of QSO absorbers

QSO name	ra	dec	z
pg0953	149.22	41.26	0.23
ton28	151.01	28.93	0.3297
3c249	165.52	-1.27	1.554
pg1116	169.79	21.32	0.1765
pg1211	183.57	14.05	0.089
pg1216	184.84	6.64	0.3313
3c273	187.28	2.05	0.158339
pg1259	195.30	59.04	0.4778
ngc5548	214.50	25.14	0.017175
mrk1383	217.28	1.29	0.08647
pg1444	221.69	40.59	0.2673

absorbers from seven systems with $cz < 10{,}500$ km s^{-1} and matching with the CfA2 Redshift Survey (Geller & Huchra 1989) they found that nearby, low column density (log $N_{HI} \lesssim 14$) absorbers are spatially distributed at random, and not correlated with the large scale structure.

In this study, we use a much larger sample of Lyα absorbers (119) to examine the relationship of neutral HI gas with the large scale void structure of the local Universe to determine the spatial distribution of Lyα absorbers. Our goal is to determine the distribution of observed Lyα absorbers within the large scale structure, specifically its abundance in voids compared to filaments. We compare our results with predictions from simulations that these absorbers live in the dense cosmic filaments that contain most of the galaxies in the Universe.

6.5 Data

We use a collection of 30 QSO absorption line systems from STIS/G140M and the main galaxy sample of SDSS DR7. Within the sky coverage of SDSS DR7, we find 11 QSO absorption line systems (seen in table 6.1) which correspond to 119 absorbers with $z < 0.107$.

6.5.1 STIS

The Space Telescope Imaging Spectrograph is a ultraviolet spectrograph on the Hubble Space Telescope. It has a high-resolution spectrograph with capabilities down to 1150Å. This is especially useful for capturing the Lyα line at rest frame 1216Å. We use the 30 absorption line systems described in Danforth and Shull [2008].

6.5.2 SDSS

We use the SDSS Data Release 7 (DR7) [Abazajian et al., 2009] sample of galaxies. The SDSS is a photometric and spectroscopic survey that covers 8,032 square degrees of the northern sky. Observations were carried out using the 2.5m telescope at Apache Point Observatory in New Mexico in five photometric bands: u, g, r, i, and z [Fukugita et al., 1996, Gunn et al., 1998]. Follow up spectroscopy was carried out for galaxies with Petrosian r band magnitude $r < 17.77$ after each photometric image was reduced, calibrated and classified [Lupton et al., 2001, 1999, Strauss et al., 2002].

Spectra were taken using circular fiber plugs with an angular size of approximately 55 arc seconds. If two galaxies were closer than this, we could only obtain the spectra of one; the other object is omitted unless there is plate overlap. Blanton et al. [2003] addresses the issue of fiber collisions by assessing the relation between physical location of the galaxy and photometric and spectroscopic properties and assigns a redshift to the object missed by SDSS.

We use the Korea Institute for Advanced Study Value-Added Galaxy Catalog (KIAS-VAGC) [Choi et al., 2010]. Its main source is the New York University Value-Added Galaxy Catalog (NYU-VAGC) Large Scale Structure Sample (brvoid0) [Blanton et al., 2005] which includes 583,946 galaxies with $10 < r \leq 17.6$. After removing 929 objects that were errors, mostly deblended outlying parts of large galaxies, including 10,497 galaxies excluded by SDSS but that were part of UZC, PSCz, RC3, or 2dF, and also including 114,303 galaxies with $17.6 < m_r < 17.77$ from NYU-VAGC (full0), there is a total of 707,817 galaxies. This catalog offers an extended magnitude range with high completeness from $10 < r < 17.6$. Additionally, we use the large scale structure void catalog from Pan et al. [2011]. This catalog contains 1054 statistically significant voids with r $> 10\ h^{-1}$ Mpc, and 79,947 void galaxies with SDSS spectroscopy in the northern galactic hemisphere.

6.6 Method

6.6.1 Location of Absorbers

For each absorber we determine whether or not it lives in a void using the void sample from Pan et al. [2011]. We find that 87 of the 119 absorbers that lie within the SDSS main sample volume reside in voids. This implies that there is a preference for Lyα absorbers to live in voids because over 70% of the absorbers live in voids where there are only 10% of the galaxies. Looking at the specific location of the absorbers within the voids as seen in figure 6.3, we see that absorbers actually prefer to reside towards the centers of the voids. The large scale structure distribution results were seen in Grogin and Geller [1998], but the void distribution was not measured.

6.6.2 Matching Galaxies

For each Lyα absorber we calculate the projected sky distance to the nearest neighbor SDSS galaxy. We also impose a maximum redshift difference of $\Delta z < 0.001$, this corresponds to a radial velocity dispersion of approximately 300 km/s. We find 53 Lyα absorbers match to a SDSS galaxy with projected sky distance $< 1\ h^{-1}$ Mpc. They are pockets of neutral HI gas in the dark matter halo of its host galaxy. We find that 31 of the 53 Lyα absorber matched galaxies (58%) are void galaxies. Figure 6.2 shows a slice of SDSS with the line of sight to a single quasar. The locations of Lyα absorbers are marked on the plot, we can see absorbers distributed throughout the entire line of sight.

6.6.3 Column Density

Figure 6.4 shows the distribution of column densities for absorbers. The distribution for both the wall absorbers as well as the void absorbers can be seen. There is no significant difference in the column densities of void absorbers. In Figure 6.5 we plot the distribution of absorbers versus distance from the nearest galaxy, and in Figure 6.6 we plot the distribution of column densities for absorbers versus the projected distance to the nearest galaxy. There is no difference in the distribution of column densities versus the projected distance to the nearest galaxy, nor is there a significant difference in the distribution of absorbers versus the projected distance to the nearest galaxy.

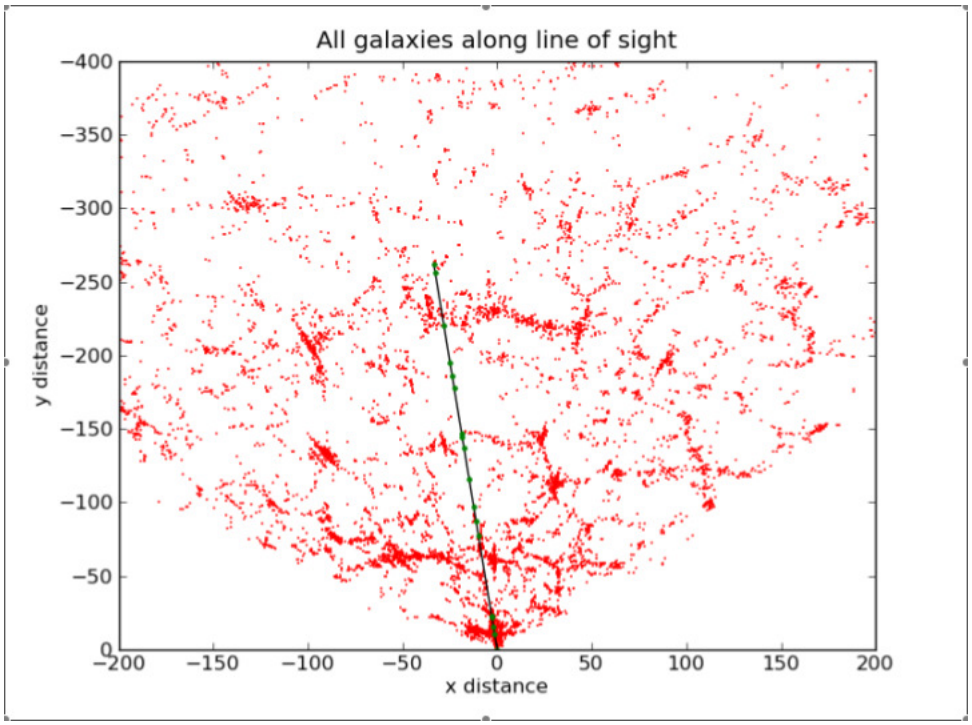

Figure 6.2: The location of Lyα absorbers are plotted along with the line of sight to the quasar that contains the absorption line in the spectrum. Absorbers are distributed along the line of sight, and there appears to be no direct correlation between the clumping of galaxies along the line of sight with the locations of the absorbers.

6.7 Results

We find the surprising result that while the Lyα absorbers detected in both large scale voids and walls seem similar in both distance from nearest galaxy as well as column density, there is a distinct preference for absorbers to be detected inside the voids, especially towards the centers of voids. Modern simulations such as those seen in Davé et al. [2001], Smith et al. [2010] are typically done on boxes $50\ h^{-1}$ Mpc on a side, which is too small for large scale structure. We also find that the Lyα absorbers should not be considered to be tracers of the filamentary structure as proposed in Cen and Ostriker [1999]. Grogin and Geller [1998] found that Lyα absorbers are not tracing the nearby large scale structure marked by typical luminous galaxies. We find that the absorbers are not randomly distributed in the nearby Universe as they found, but rather they have a preference to reside towards the centers of the most underdense structures in the Universe. This agrees with predictions from Carswell and Rees [1987] that voids can not be deficient in Lyα clouds unless they

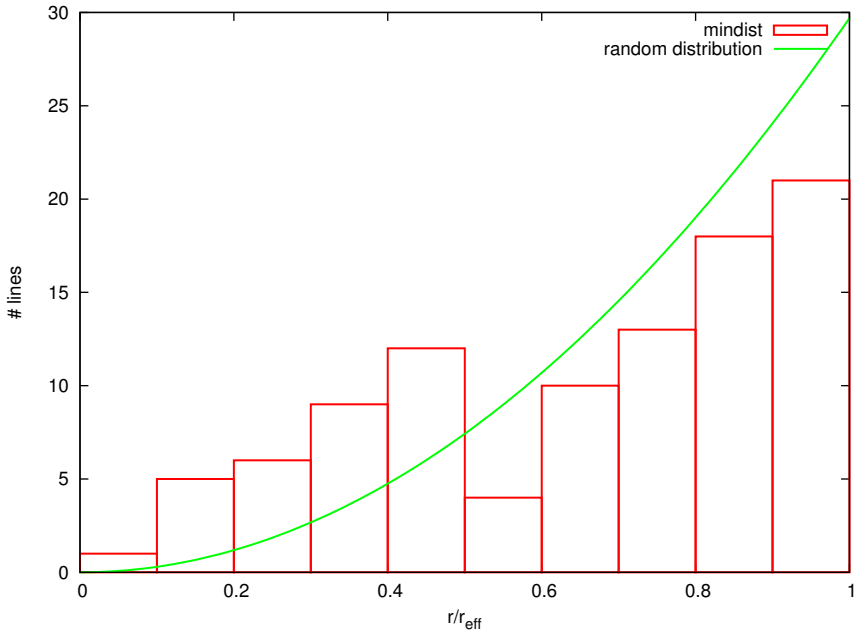

Figure 6.3: A histogram of the number of Lyα absorbers as a function of the ratio of the distance from the center of the void it is located in versus the radius of the void. Overplotted is the line of a random distribution of absorbers inside the voids with N(r) $\propto$ r^2. We see that there is a clear preference for the absorbers to reside closer to the center of the voids in an environment of extremely low density ($\delta <$ -0.9).

occupied $<$ 5% of the cosmic volume.

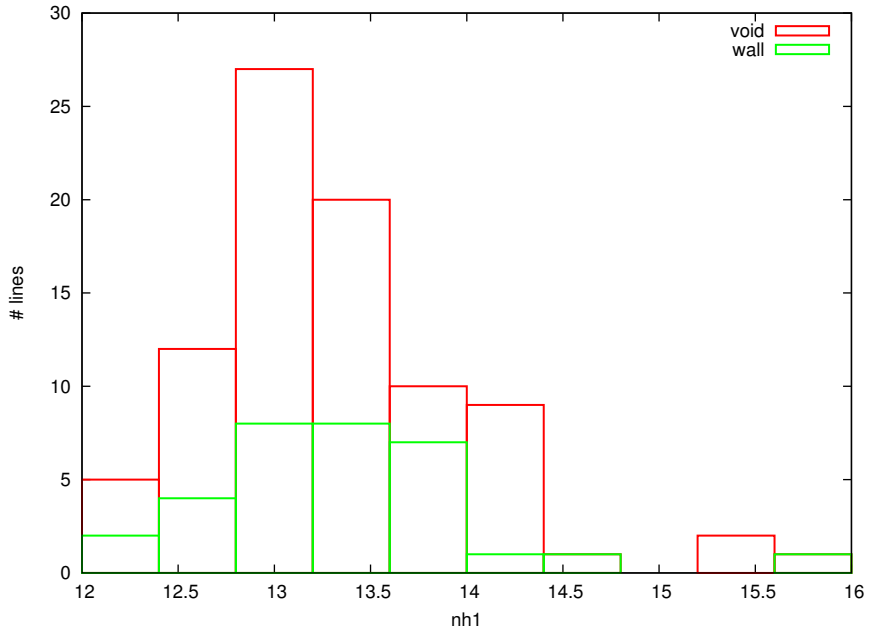

Figure 6.4: A histogram of the column densities of the Lyα absorbers. We see that the distribution for both the wall and void absorbers are similar and the absorbers span the entire range of the sample obtained from HST STIS.

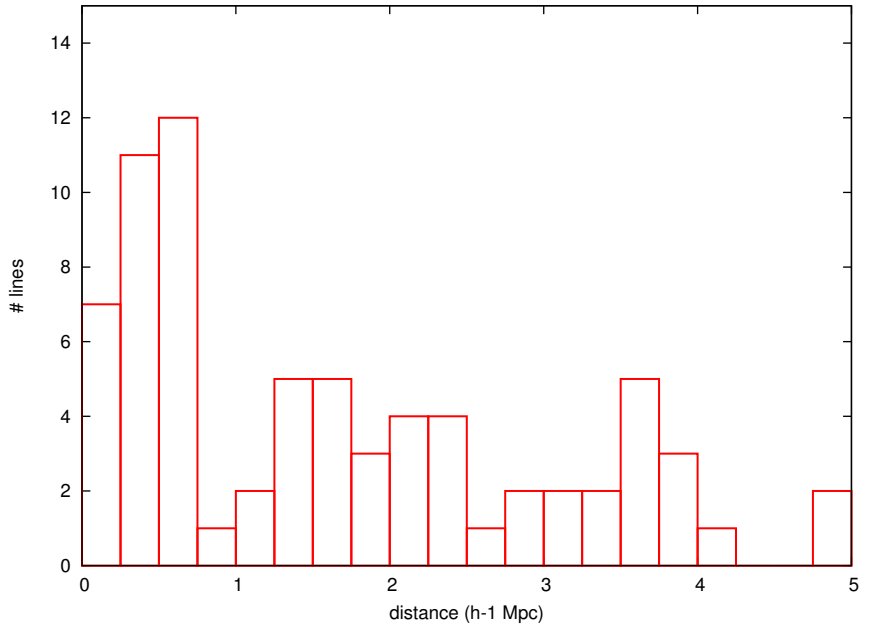

Figure 6.5: A histogram of the number of Lyα absorbers as a function of its projected distance from the nearest galaxy. We see that many absorbers have a galaxy matched closer than 1 h^{-1} Mpc in projected distance. Beyond 1 h^{-1} Mpc, the distribution of "match" galaxy projected distance is flat.

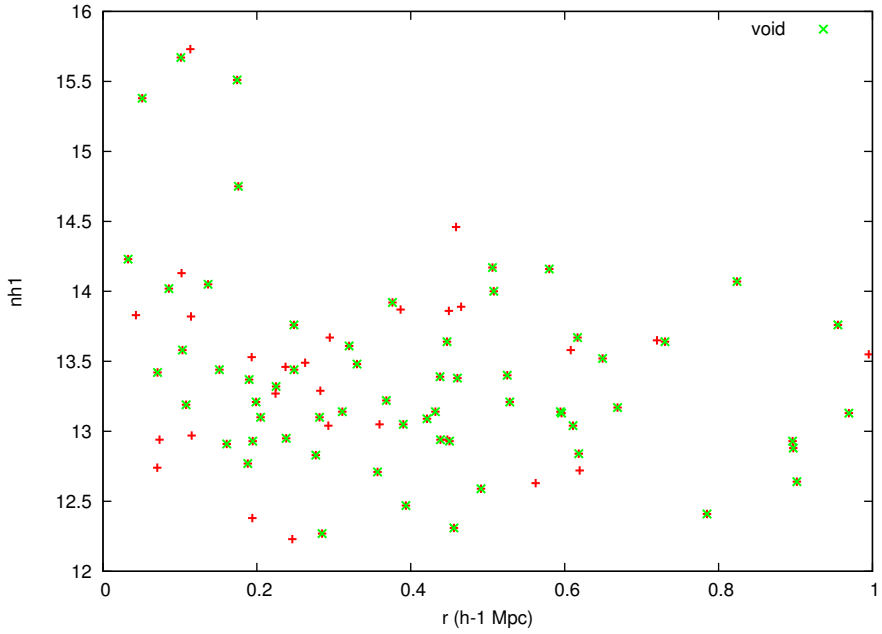

Figure 6.6: This plot shows the distribution of column densities versus the projected distance from the nearest galaxy. We see that the distribution for wall and void absorbers are similar. There is no preference for void absorbers to have higher column densities at larger radii from the host galaxy.

Chapter 7

Conclusion/Future Work

7.1 Results from Void Catalog

In chapter 2, we studied the distribution of cosmic voids and void galaxies using Sloan Digital Sky Survey data release 7 using an absolute magnitude cut of $M_r < -20.09$. Using the VoidFinder algorithm as described by Hoyle and Vogeley [2002], we identify 1054 statistically significant voids in the northern galactic hemisphere greater than 10 h^{-1} Mpc in radius, covering 62% of the volume. There are 8,046 galaxies brighter than $M_r = -20.09$ that lie within the voids, accounting for approximately 6% of the galaxies, and 79,947 void galaxies (11.3%) with $m_r < 17.6$. The largest void is just over 30 h^{-1} Mpc in effective radius. The median effective radius is 17 h^{-1} Mpc. Voids of size $r_{eff} \sim 20h^{-1}$ Mpc dominate the void volume. The voids are found to be significantly underdense, with $\delta < -0.85$ near the edges of the voids. We tested the sensitivity of the void finding algorithm to changes in the absolute magnitude cut within the range $-19.6 > M_r > -20.6$. The resulting void regions are largely similar with slight differences only near the edges of the void regions. The radial density profiles of the voids are found to be similar to predictions of dynamically distinct underdensities in gravitational theory. We compared the results of VoidFinder on SDSS DR7 to mock catalogs generated from a SPH halo model simulation as well as other Λ-CDM simulations and found similar results, ruling out inconsistencies resulting from selection bias and survey geometry.

Expanding on this result, we tested the void finding algorithm on alternative surveys and cosmo-

logical simulations in chapter 3, and compared it to another void finding algorithm that recreates the density field [Platen et al., 2008]. We find that VoidFinder is robust enough to work with different sets of data and different cosmological simulations. Using 21,641 volume limited catalog galaxies over 25,000 square degrees of the souther sky, VoidFinder finds 219 voids with r $> 10\ h^{-1}$ Mpc, average $r_{eff} = 17.86\ h^{-1}$ Mpc, and 1,296 volume limited void galaxies in 6dF. VoidFinder voids agree with void findings results from the Watershed Void Finder and the Böotes "supervoid" was identified in both void finders as a collection of smaller voids. Various cosmological simulations are able to reproduce the large scale structure void properties observed with SDSS.

7.1.1 Future Work

Throughout the literature search on voids and void galaxies there is usually one thing in common. The astronomical community does not yet have a full definition for what constitutes a void or what constitutes a void galaxy. There is an entire separate branch of galaxy study that focuses on "isolated" galaxies, these are galaxies that have no local environment neighbors, yet in the literature, these galaxies are often referred to as void galaxies as well. Colberg et al. [2008] attempted to address the issue of unifying void finding algorithms after a series of international collaboration meetings in Aspen and Amsterdam brought together the leading researchers in large scale void structures. The meeting was successful in that like minds came together to explore and discuss the implications of void studies and the field as a whole gained a better understanding of the amount of ongoing observational and theoretical work. However, there continues to be individual void definitions that are best fitting to individual studies. Each individual void definition may be the most fitting for that particular study, but there needs to be a well defined set of nomenclature rules for void catalogs that are released to the public. The void catalog released in the work of this thesis is a galaxy based cosmic void catalog.

There is a lot of work that can still be done to expand void catalogs. Already there are new Sloan data releases and with upcoming surveys such as LSST and SKA, there is plenty of data to be mined. While the specific void finding algorithm may not be optimal for use on these new data releases, similar algorithms can be modified to work. Void finding has been and will be a useful tool

for assessing the cosmology and physics of the Universe.

7.2 Results from Void Shapes

In chapter 4, we determined that voids are generally spherical in shape, with no major deviation for being highly elliptical. This is expected as we expect large scale voids to become more spherical over time. Similar results can be seen in void shape analysis done by Foster and Nelson [2009] on a subsample of voids from SDSS DR5. Figure 4.4 shows a slice of SDSS with the comparison of a best fit ellipsoid plotted against the maximal sphere of the void region. The best fit ellipsoid appears to fill in the void volume much better than the maximal sphere, it also preserves the volume of the void region. The results of void ellipticity in the void catalog can be seen in Figure 4.5. The three axes of the ellipsoid, $a \geq b \geq c$, can be described by the two ratios b/a and c/b. We can see that there appears to be a slight preference for the ellipsoidal void regions to have a prolate shape as opposed to an oblate shape. Prolateness can be seen in the figure as an excess of points with smaller b/a compared to c/b. Oblateness is seen as an excess of points with smaller c/b compared to b/a A similar result can be seen (Figure 4.6) when looking at voids in real versus redshift space using the mock simulations described in a previous section. This means that the excess prolateness is not caused by redshift space distortions. It is likely due to a preference for voids to merge in pairs for the resulting observed void to be a prolate ellipsoid.

7.2.1 Future Work

More analysis into the substructure of voids needs to be done to determine the causes of the void ellipticity measured in SDSS voids. Ryden and Melott [1996] measured appreciable increases in both the size and shape of voids by measuring the void probability function (VPF) and underdense probability function (UPF) of voids in simulated real and redshift space. They also measured a preference for alignment along the line of sight, results that are not measured in larger simulations since then, and in the observed SDSS Universe. There have been numerous studies into the shapes and structure in the interior of voids [Sahni et al., 1998, Gottlöber et al., 2003], as well as the filamentary structure of the Universe [Aragon-Calvo et al., 2010, Noh and Cohn, 2011]. More

comprehensive study of the interior distribution of galaxies within voids will help us understand the effects of redshift space distortions as well as the effects of cosmology on large scale structure.

7.3 Void Galaxy Distribution

In chapter 5, we sought to understand the distribution of galaxies in the observed Universe. By measuring the small scale structure of cosmic voids, we can better understand cosmology within voids. We consider voids to be mini-universes with differing cosmological parameters, primarily Ω_m, Ω_Λ, and σ_8 [Goldberg et al., 2005].

We found void galaxies are less clustered than their wall counterparts, with $s_0 = 7.8$ and $\gamma = 1.2$ assuming the correlation equation has the form $\xi = (s/s_0)^{-\gamma}$. This is similar in comparison to work done by Abbas and Sheth [2006] which compared galaxies living in low density regions ($< 33\%$ mean density) versus their wall counterparts.

7.3.1 Future Work

There is still a lot to be gained from studying the small scale structure of voids. The void environment gives us a testbed for determining the accuracy of predictions from models of cosmology. The standard model of cosmology, ΛCDM, predicts specific properties to the distribution of matter within voids. We can use studies of galaxies in voids in 2 separate ways using a suite of cosmological simulations, such as the Cosmic Calibration suite of simulations [Heitmann et al., 2006, Habib et al., 2007].

First, we can study the accuracy of cosmological simulations in determining the small scale structure of voids. This is done by allowing the cosmological parameters to vary in full cosmological simulations and then looking at the void galaxy distribution results in comparison to the SDSS observational results found in this thesis.

Second, we can test cosmological theories that predict the small scale void environments. By treating voids as underdense Universes, we allow cosmological parameters to vary in simulations targeted specifically at reproducing the galaxy distribution within voids. The simulation with galaxy distributions that best match the void galaxies from SDSS tells us what the cosmology is within

voids.

7.4 Results from Lyα Absorbers in Voids

In chapter 6, we find that while the Lyα absorbers detected in both large scale voids and walls seem similar in both distance from nearest galaxy as well as column density, there is a distinct preference for absorbers to be detected inside the voids, especially towards the centers of voids. This is a surprising results becasue modern simulations such as those seen in Davé et al. [2001], Smith et al. [2010] are typically done on boxes $50\ h^{-1}$ Mpc on a side, which is too small for large scale structure. We also find that the Lyα absorbers should not be considered to be tracers of the filamentary structure as proposed in Cen and Ostriker [1999]. Grogin and Geller [1998] found that Lyα absorbers are not tracing the nearby large scale structure marked by typical luminous galaxies. We find that the absorbers are not randomly distributed in the nearby Universe as they found, but rather they have a preference to reside towards the centers of the most underdense structures in the Universe. This agrees with predictions from Carswell and Rees [1987] that voids can not be deficient in Lyα clouds unless they occupied $< 5\%$ of the cosmic volume.

7.4.1 Future Work

With the results found in this thesis, the push is on theorists to run numerical simulations on volumes that contain large underdense void regions to determine the spatial distribution of Lyα clouds. The next step for observational results is to compare HST FUSE results to HST Cosmic Origins Spectrograph (COS) results. Most of COS data has been taken at the time of writing of this thesis, it will expand the number of absorbers to compare from 11 to approximately 50. If additional void catalogs are considered, all COS QAL systems can be considered, giving us a data sample of almost 1,000 absorption lines. With the increased number of absorbers and increased volume coverage, it will be possible to conduct cross correlations of Lyα absorbers with large scale structure, pinning down the spatial distribution of these absorbers. It will also be possible to cross correlate Lyα absorbers with galaxy types. We can use the locations of neutral HI clouds to determine the properties of galaxy and filament gas environments.

Using Lyα absorbers associated with void galaxies, HST spectra also contains information for metal lines, primarily OVI lines as done in Stocke et al. [2007] for isolated galaxies. The metal properties of void galaxies is of particular interest because there is not expected to be many heavier metals in voids due to the lower mass densities in voids and the lack of interactions and mergers that produce metals.

7.5 Final Discussion

Research in cosmic voids is an active and growing field. As we continue to learn more about the Universe, the focus on large scale structure has grown. We are entering an era now where large telescopic surveys can finally allow us to prod and observe the three dimensional structure of the Universe. Studying large scale structure can provide us with insight into various aspects of astronomy and physics. On large scales, the distribution of voids and filaments describe the cosmology of the Universe. On a smaller scale, the contents and environments of void galaxies describe the evolution of galaxies, with underdense void regions providing a pristine test environment for growth. Study of large scale voids will play an important part in enhancing our understanding of cosmology and help assess the plausibility of cosmological models, including accepting or rejecting ΛCDM.

Bibliography

Kevork N Abazajian, Jennifer K Adelman-McCarthy, Marcel A Agüeros, Sahar S Allam, Carlos Allende Prieto, Deokkeun An, Kurt S. J Anderson, Scott F Anderson, James Annis, Neta A Bahcall, C. A. L Bailer-Jones, J. C Barentine, Bruce A Bassett, Andrew C Becker, Timothy C Beers, Eric F Bell, Vasily Belokurov, Andreas A Berlind, Eileen F Berman, Mariangela Bernardi, Steven J Bickerton, Dmitry Bizyaev, John P Blakeslee, Michael R Blanton, John J Bochanski, William N Boroski, Howard J Brewington, Jarle Brinchmann, J Brinkmann, Robert J Brunner, Tamás Budavári, Larry N Carey, and Samuel Carliles. The seventh data release of the sloan digital sky survey. *The Astrophysical Journal Supplement*, 182:543, Jun 2009. doi: 10.1088/0067-0049/182/2/543.

Ummi Abbas and Ravi K Sheth. The environmental dependence of galaxy clustering in the sloan digital sky survey. *Monthly Notices of the Royal Astronomical Society*, 372:1749, Nov 2006. doi: 10.1111/j.1365-2966.2006.10987.x.

J Aikio and P Maehoenen. A simple void-searching algorithm. *Astrophysical Journal v.497*, 497: 534, Apr 1998. doi: 10.1086/305509.

M. A Aragon-Calvo, R van de Weygaert, P. A Araya-Melo, E Platen, and A. S Szalay. Unfolding the hierarchy of voids. *Monthly Notices of the Royal Astronomical Society: Letters*, 404:L89, May 2010. doi: 10.1111/j.1745-3933.2010.00841.x.

A. J Benson, Fiona Hoyle, Fernando Torres, and Michael S Vogeley. Galaxy voids in cold dark matter universes. *Monthly Notice of the Royal Astronomical Society*, 340:160, Mar 2003. doi: 10.1046/j.1365-8711.2003.06281.x.

E Bertschinger. The self-similar evolution of holes in an einstein-de sitter universe. *Astrophysical Journal Supplement Series (ISSN 0067-0049)*, 58:1, May 1985. doi: 10.1086/191027.

Rahul Biswas, Esfandiar Alizadeh, and Benjamin D Wandelt. Voids as a precision probe of dark energy. *Physical Review D*, 82:23002, Jul 2010. doi: 10.1103/PhysRevD.82.023002. (c) 2010: The American Physical Society.

Michael R Blanton, Huan Lin, Robert H Lupton, F. Miller Maley, Neal Young, Idit Zehavi, and Jon Loveday. An efficient targeting strategy for multiobject spectrograph surveys: the sloan digital sky survey "tiling" algorithm. *The Astronomical Journal*, 125:2276, Apr 2003. doi: 10.1086/344761.

Michael R Blanton, David J Schlegel, Michael A Strauss, J Brinkmann, Douglas Finkbeiner, Masataka Fukugita, James E Gunn, David W Hogg, Željko Ivezić, G. R Knapp, Robert H Lupton, Jeffrey A Munn, Donald P Schneider, Max Tegmark, and Idit Zehavi. New york university value-added galaxy catalog: A galaxy catalog based on new public surveys. *The Astronomical Journal*, 129:2562, Jun 2005. doi: 10.1086/429803. (c) 2005: The American Astronomical Society.

G. R Blumenthal, L. N da Costa, D. S Goldwirth, M Lecar, and T Piran. The largest possible voids. *Astrophysical Journal*, 388:234, Apr 1992. doi: 10.1086/171147.

J. Richard Bond, Lev Kofman, and Dmitry Pogosyan. How filaments of galaxies are woven into the cosmic web. *Nature*, 380:603, Apr 1996. doi: 10.1038/380603a0. (c) 1996: Nature.

P. D Bristow and S Phillipps. On the baryon content of the universe. *R.A.S. MONTHLY NOTICES V.267*, 267:13, Mar 1994.

Scott Burles and David Tytler. The neutral hydrogen column density towards q1937-1009 from the unabsorbed intrinsic continuum in the lyman-alpha forest. *The Astronomical Journal*, 114:1330, Oct 1997. doi: 10.1086/118566.

R. F Carswell and M. J Rees. Constraints on voids at high redshifts from ly-alpha absorbers. *Royal Astronomical Society*, 224:13P, Jan 1987.

L Ceccarelli, N. D Padilla, C Valotto, and D. G Lambas. Voids in the 2dfgrs and cdm simulations: spatial and dynamical properties. *Monthly Notices of the Royal Astronomical Society*, 373:1440, Dec 2006. doi: 10.1111/j.1365-2966.2006.11129.x.

L Ceccarelli, N Padilla, and D. G Lambas. Large-scale modulation of star formation in void walls. *Monthly Notices of the Royal Astronomical Society: Letters*, 390:L9, Oct 2008. doi: 10.1111/j.1745-3933.2008.00520.x. (c) Journal compilation © 2008 RAS.

Renyue Cen and Jeremiah P Ostriker. Where are the baryons? *The Astrophysical Journal*, 514:1, Mar 1999. doi: 10.1086/306949.

Renyue Cen and Jeremiah P Ostriker. Where are the baryons? ii. feedback effects. *The Astrophysical Journal*, 650:560, Oct 2006. doi: 10.1086/506505.

Yun-Young Choi, Du-Hwan Han, and Sungsoo S Kim. Korea institute for advanced study value-added galaxy catalog. *Journal of the Korean Astronomical Society*, 43:191, Dec 2010. (c) Korean Astronomical Society.

Sirichai Chongchitnan and Joseph Silk. A study of high-order non-gaussianity with applications to massive clusters and large voids. *The Astrophysical Journal*, 724:285, Nov 2010. doi: 10.1088/0004-637X/724/1/285.

Jörg M Colberg, Ravi K Sheth, Antonaldo Diaferio, Liang Gao, and Naoki Yoshida. Voids in a cdm universe. *Monthly Notices of the Royal Astronomical Society*, 360:216, Jun 2005. doi: 10.1111/j.1365-2966.2005.09064.x.

Jörg M Colberg, Frazer Pearce, Caroline Foster, Erwin Platen, Riccardo Brunino, Mark Neyrinck, Spyros Basilakos, Anthony Fairall, Hume Feldman, Stefan Gottlöber, Oliver Hahn, Fiona Hoyle, Volker Müller, Lorne Nelson, Manolis Plionis, Cristiano Porciani, Sergei Shandarin, Michael S Vogeley, and Rien van de Weygaert. The aspen-amsterdam void finder comparison project. *Monthly Notices of the Royal Astronomical Society*, 387:933, Jun 2008. doi: 10.1111/j.1365-2966.2008.13307.x. (c) Journal compilation © 2008 RAS.

Matthew Colless, Gavin Dalton, Steve Maddox, Will Sutherland, Peder Norberg, Shaun Cole, Joss Bland-Hawthorn, Terry Bridges, Russell Cannon, Chris Collins, Warrick Couch, Nicholas Cross, Kathryn Deeley, Roberto De Propris, Simon P Driver, George Efstathiou, Richard S Ellis, Carlos S Frenk, Karl Glazebrook, Carole Jackson, Ofer Lahav, Ian Lewis, Stuart Lumsden, Darren Madgwick, John A Peacock, Bruce A Peterson, Ian Price, Mark Seaborne, and Keith Taylor. The 2df galaxy redshift survey: spectra and redshifts. *Monthly Notices of the Royal Astronomical Society*, 328:1039, Dec 2001. doi: 10.1046/j.1365-8711.2001.04902.x.

Anca Constantin and Michael S Vogeley. The clustering of low-luminosity active galactic nuclei. *The Astrophysical Journal*, 650:727, Oct 2006. doi: 10.1086/507087.

L. Nicolaci da Costa, P. S Pellegrini, W. L. W Sargent, J Tonry, M Davis, A Meiksin, David W Latham, J. W Menzies, and I. A Coulson. The southern sky redshift survey. *Astrophysical Journal*, 327:544, Apr 1988. doi: 10.1086/166215.

Guido D'Amico, Marcello Musso, Jorge Noreña, and Aseem Paranjape. Excursion sets and non-gaussian void statistics. *Physical Review D*, 83(2):23521–23521, Jan 1. doi: doi:10.1103/PhysRevD.83.023521.

Charles W Danforth and J. Michael Shull. The low-z intergalactic medium. i. o vi baryon census. *The Astrophysical Journal*, 624:555, May 2005. doi: 10.1086/429285.

Charles W Danforth and J. Michael Shull. The low-z intergalactic medium. iii. h i and metal absorbers at z ¡ 0.4. *The Astrophysical Journal*, 679:194, May 2008. doi: 10.1086/587127.

Charles W Danforth, J. Michael Shull, Jessica L Rosenberg, and John T Stocke. The low-z intergalactic medium. ii. ly, o vi, and c iii forest. *The Astrophysical Journal*, 640:716, Apr 2006. doi: 10.1086/500191.

Romeel Davé, S. R Heap, G. M Williger, R. J Weymann, T. M Tripp, and E. B Jenkins. The metallicity of the local igm from the hst/stis spectrum of 3c273. *eprint arXiv*, page 9242, Sep 2001.

M Davis and P. J. E Peebles. A survey of galaxy redshifts. v - the two-point position and velocity correlations. *Astrophysical Journal*, 267:465, Apr 1983. doi: 10.1086/160884.

V de Lapparent, M. J Geller, and J. P Huchra. A slice of the universe. *Astrophysical Journal*, 302: L1, Mar 1986. doi: 10.1086/184625.

A Dekel. Superclusters as nondissipative pancakes - flattening. *Astrophysical Journal*, 264:373, Jan 1983. doi: 10.1086/160605.

John Dubinski, L. N da Costa, D. S Goldwirth, M Lecar, and T Piran. Void evolution and the large-scale structure. *Astrophysical Journal*, 410:458, Jun 1993. doi: 10.1086/172762.

H El-Ad and T Piran. A case devoid of bias: Optical redshift survey voids versus iras voids. *Monthly Notices of the Royal Astronomical Society*, 313:553, Apr 2000. doi: 10.1046/j.1365-8711.2000.03286.x.

H El-Ad, T Piran, and L. N Dacosta. A catalogue of the voids in the iras 1.2-jy survey. *Monthly Notices of the Royal Astronomical Society*, 287:790, Jun 1997.

Hagai El-Ad and Tsvi Piran. Voids in the large-scale structure. *Astrophysical Journal v.491*, 491: 421, Dec 1997. doi: 10.1086/304973.

J. A Fillmore and P Goldreich. Self-similar spherical voids in an expanding universe. *Astrophysical Journal*, 281:9, Jun 1984. doi: 10.1086/162071.

Karl B Fisher, John P Huchra, Michael A Strauss, Marc Davis, Amos Yahil, and David Schlegel. The iras 1.2 jy survey: Redshift data. *Astrophysical Journal Supplement v.100*, 100:69, Sep 1995. doi: 10.1086/192208.

Caroline Foster and Lorne A Nelson. The size, shape, and orientation of cosmological voids in the sloan digital sky survey. *The Astrophysical Journal*, 699:1252, Jul 2009. doi: 10.1088/0004-637X/699/2/1252.

M Fukugita, T Ichikawa, J. E Gunn, M Doi, K Shimasaku, and D. P Schneider. The sloan digital sky survey photometric system. *Astronomical Journal v.111*, 111:1748, Apr 1996. doi: 10.1086/117915.

M Fukugita, C. J Hogan, and P. J. E Peebles. The cosmic baryon budget. *Astrophysical Journal v.503*, 503:518, Aug 1998. doi: 10.1086/306025. (c) 1998: The American Astronomical Society.

Masataka Fukugita and P. J. E Peebles. The cosmic energy inventory. *The Astrophysical Journal*, 616:643, Dec 2004. doi: 10.1086/425155.

Steven R Furlanetto and Tsvi Piran. The evidence of absence: galaxy voids in the excursion set formalism. *Monthly Notices of the Royal Astronomical Society*, 366:467, Feb 2006. doi: 10.1111/j.1365-2966.2005.09862.x.

Liang Gao and Simon D. M White. Assembly bias in the clustering of dark matter haloes. *Monthly Notices of the Royal Astronomical Society: Letters*, 377:L5, Apr 2007. doi: 10.1111/j.1745-3933.2007.00292.x.

Margaret J Geller and John P Huchra. Mapping the universe. *Science (ISSN 0036-8075)*, 246:897, Nov 1989. doi: 10.1126/science.246.4932.897.

R Giovanelli and M. P Haynes. A 21 cm survey of the pisces-perseus supercluster. i - the declination zone +27.5 to +33.5 degrees. *Astronomical Journal (ISSN 0004-6256)*, 90:2445, Dec 1985. doi: 10.1086/113949.

David M Goldberg, Timothy D Jones, Fiona Hoyle, Randall R Rojas, Michael S Vogeley, and Michael R Blanton. The mass function of void galaxies in the sloan digital sky survey data release 2. *The Astrophysical Journal*, 621:643, Mar 2005. doi: 10.1086/427679. (c) 2005: The American Astronomical Society.

Stefan Gottlöber, Ewa L okas, Anatoly Klypin, and Yehuda Hoffman. The structure of voids. *Monthly Notices of the Royal Astronomical Society*, 344:715, Sep 2003. doi: 10.1046/j.1365-8711.2003.06850.x.

S. A Gregory and L. A Thompson. The coma/a1367 supercluster and its environs. *Astrophysical Journal*, 222:784, Jun 1978. doi: 10.1086/156198. A&AA ID. AAA021.160.059.

Norman A Grogin and Margaret J Geller. Lyalpha absorption systems and the nearby galaxy distribution. *The Astrophysical Journal*, 505:506, Oct 1998. doi: 10.1086/306208.

Norman A Grogin and Margaret J Geller. An imaging and spectroscopic survey of galaxies within prominent nearby voids. i. the sample and luminosity distribution. *The Astronomical Journal*, 118:2561, Dec 1999. doi: 10.1086/301126.

Norman A Grogin and Margaret J Geller. An imaging and spectroscopic survey of galaxies within prominent nearby voids. ii. morphologies, star formation, and faint companions. *The Astronomical Journal*, 119:32, Jan 2000. doi: 10.1086/301179.

J. E Gunn, M Carr, C Rockosi, M Sekiguchi, K Berry, B Elms, E de Haas, Ž Ivezić, G Knapp, R Lupton, G Pauls, R Simcoe, R Hirsch, D Sanford, S Wang, D York, F Harris, J Annis, L Bartozek, W Boroski, J Bakken, M Haldeman, S Kent, S Holm, D Holmgren, D Petravick, A Prosapio, R Rechenmacher, M Doi, M Fukugita, K Shimasaku, N Okada, C Hull, W Siegmund, E Mannery, M Blouke, D Heidtman, D Schneider, R Lucinio, and J Brinkman. The sloan digital sky survey photometric camera. *The Astronomical Journal*, 116:3040, Dec 1998. doi: 10.1086/300645.

Salman Habib, Katrin Heitmann, David Higdon, Charles Nakhleh, and Brian Williams. Cosmic calibration: Constraints from the matter power spectrum and the cosmic microwave background. *Physical Review D*, 76:83503, Oct 2007. doi: 10.1103/PhysRevD.76.083503.

M. A Hausman, D. W Olson, and B. D Roth. The evolution of voids in the expanding universe. *Astrophysical Journal*, 270:351, Jul 1983. doi: 10.1086/161128.

M. P Haynes. H i cosmology in the local universe with alfalfa. *Frontiers of Astrophysics: A Celebration of NRAO's 50th Anniversary ASP Conference Series*, 395:125, Aug 2008.

Katrin Heitmann, David Higdon, Charles Nakhleh, and Salman Habib. Cosmic calibration. *The Astrophysical Journal*, 646:L1, Jul 2006. doi: 10.1086/506448.

G. L Hoffman, E. E Salpeter, and I Wasserman. Spherical simulations of holes and honeycombs in friedmann universes. *Astrophysical Journal*, 268:527, May 1983. doi: 10.1086/160976.

Y Hoffman and J Shaham. On the origin of the voids in the galaxy distribution. *Astrophysical Journal*, 262:L23, Nov 1982. doi: 10.1086/183904. A&AA ID. AAA032.160.054.

Fiona Hoyle and Michael S Vogeley. Voids in the point source catalogue survey and the updated zwicky catalog. *The Astrophysical Journal*, 566:641, Feb 2002. doi: 10.1086/338340.

Fiona Hoyle and Michael S Vogeley. Voids in the two-degree field galaxy redshift survey. *The Astrophysical Journal*, 607:751, Jun 2004. doi: 10.1086/386279. (c) 2004: The American Astronomical Society.

Fiona Hoyle, Randall R Rojas, Michael S Vogeley, and Jon Brinkmann. The luminosity function of void galaxies in the sloan digital sky survey. *The Astrophysical Journal*, 620:618, Feb 2005. doi: 10.1086/427176. (c) 2005: The American Astronomical Society.

Esther M Hu, Tae-Sun Kim, Lennox L Cowie, Antoinette Songaila, and Michael Rauch. The distribution of column densities and b values in the lyman-alpha forest. *Astronomical Journal v.110*, 110:1526, Oct 1995. doi: 10.1086/117625.

J Huchra, M Davis, D Latham, and J Tonry. A survey of galaxy redshifts. iv - the data. *Astrophysical Journal Supplement Series (ISSN 0067-0049)*, 52:89, Jun 1983. doi: 10.1086/190860.

Lam Hui, Alberto Nicolis, and Christopher W Stubbs. Equivalence principle implications of modified gravity models. *Physical Review D*, 80:104002, Nov 2009. doi: 10.1103/PhysRevD.80.104002.

V Icke. Voids and filaments. *Royal Astronomical Society*, 206:1P, Jan 1984.

Hannah Jang-Condell and Lars Hernquist. First structure formation: A simulation of small-scale structure at high redshift. *The Astrophysical Journal*, 548:68, Feb 2001. doi: 10.1086/318674.

N Jarosik, C. L Bennett, J Dunkley, B Gold, M. R Greason, M Halpern, R. S Hill, G Hinshaw, A Kogut, E Komatsu, D Larson, M Limon, S. S Meyer, M. R Nolta, N Odegard, L Page, K. M Smith, D. N Spergel, G. S Tucker, J. L Weiland, E Wollack, and E. L Wright. Seven-year wilkinson microwave anisotropy probe (wmap) observations: Sky maps, systematic errors, and basic results. *The Astrophysical Journal Supplement*, 192:14, Feb 2011. doi: 10.1088/0067-0049/192/2/14.

Milikel Joeveer, Joan Einasto, and Erik Tago. Spatial distribution of galaxies and of clusters of galaxies in the southern galactic hemisphere. *Monthly Notices of the Royal Astronomical Society*, 185:357, Nov 1978. A&AA ID. AAA022.158.091.

D. Heath Jones, Will Saunders, Matthew Colless, Mike A Read, Quentin A Parker, Fred G Watson, Lachlan A Campbell, Daniel Burkey, Thomas Mauch, Lesa Moore, Malcolm Hartley, Paul Cass, Dionne James, Ken Russell, Kristin Fiegert, John Dawe, John Huchra, Tom Jarrett, Ofer Lahav, John Lucey, Gary A Mamon, Dominique Proust, Elaine M Sadler, and Ken ichi Wakamatsu. The 6df galaxy survey: samples, observational techniques and the first data release. *Monthly Notices of the Royal Astronomical Society*, 355:747, Dec 2004. doi: 10.1111/j.1365-2966.2004.08353.x.

Marc Kamionkowski, Licia Verde, and Raul Jimenez. The void abundance with non-gaussian primordial perturbations. *Journal of Cosmology and Astroparticle Physics*, 01:010, Jan 2009. doi: 10.1088/1475-7516/2009/01/010.

I. D. Karachentsev, D. I. Makarov, and V. E. Karachentseva. Properties of 513 Isolated Galaxies in the Local Supercluster. In L. Verdes-Montenegro, A. Del Olmo, & J. Sulentic, editor, *Astronomical Society of the Pacific Conference Series*, volume 421 of *Astronomical Society of the Pacific Conference Series*, pages 69–+, October 2010.

V. E Karachentseva. Catalogue of isolated galaxies. *Soobshch. Spets. Astrofiz. Obs.*, 8:3, Jan 1973. A&AA ID. AAA010.158.043.

G Kauffmann and A. P Fairall. Voids in the distribution of galaxies - an assessment of their significance and derivation of a void spectrum. *Royal Astronomical Society*, 248:313, Jan 1991.

Tae-Sun Kim, Esther M Hu, Lennox L Cowie, and Antoinette Songaila. The redshift evolution of the ly alpha forest. *Astronomical Journal v.114*, 114:1, Jul 1997. doi: 10.1086/118446.

R. P Kirshner, A Oemler, P. L Schechter, and S. A Shectman. A million cubic megaparsec void in bootes. *Astrophysical Journal*, 248:L57, Sep 1981. doi: 10.1086/183623. A&AA ID. AAA030.158.052.

R. P Kirshner, A Oemler, P. L Schechter, S. A Shectman, and D. L Tucker. The las campanas deep redshift survey. *2. Rencontre de Blois: 25. anniversary of the cosmic background radiation discovery - physical cosmology*, page 595, Jan 1991.

B Kuhn, U Hopp, and H Elsaesser. Results of a search for faint galaxies in voids. *Astronomy and Astrophysics*, 318:405, Feb 1997.

Stephen D Landy and Alexander S Szalay. Bias and variance of angular correlation functions. *Astrophysical Journal*, 412:64, Jul 1993. doi: 10.1086/172900.

Guilhem Lavaux and Benjamin D Wandelt. Precision cosmology with voids: definition, methods, dynamics. *Monthly Notices of the Royal Astronomical Society*, 403:1392, Apr 2010. doi: 10.1111/j.1365-2966.2010.16197.x.

Jounghun Lee and Daeseong Park. Constraining the dark energy equation of state with cosmic voids. *The Astrophysical Journal Letters*, 696:L10, May 2009. doi: 10.1088/0004-637X/696/1/L10.

U Lindner, M Einasto, J Einasto, W Freudling, K Fricke, V Lipovetsky, S Pustilnik, Y Izotov, and G Richter. The distribution of galaxies in voids. *Astronomy and Astrophysics*, 314:1, Oct 1996.

Limin Lu, Wallace L. W Sargent, Donna S Womble, and Masahide Takada-Hidai. The lyman-alpha forest at z approximately 4: Keck hires observations of q0000-26. *Astrophysical Journal v.472*, 472:509, Dec 1996. doi: 10.1086/178084.

R Lupton, J. E Gunn, Z Ivezić, G. R Knapp, and S Kent. The sdss imaging pipelines. *Astronomical Data Analysis Software and Systems X*, 238:269, Jan 2001.

Robert H Lupton, James E Gunn, and Alexander S Szalay. A modified magnitude system that produces well-behaved magnitudes, colors, and errors even for low signal-to-noise ratio measurements. *The Astronomical Journal*, 118:1406, Sep 1999. doi: 10.1086/301004.

Roger Lynds. The absorption-line spectrum of 4c 05.34. *Astrophysical Journal*, 164:L73, Mar 1971. doi: 10.1086/180695. A&AA ID. AAA005.141.064.

Piero Madau, Lucia Pozzetti, and Mark Dickinson. The star formation history of field galaxies. *Astrophysical Journal v.498*, 498:106, May 1998. doi: 10.1086/305523.

H Mathis and S. D. M White. Voids in the simulated local universe. *Monthly Notice of the Royal Astronomical Society*, 337:1193, Dec 2002. doi: 10.1046/j.1365-8711.2002.06010.x.

S Maurogordato, R Schaeffer, and L. N da Costa. The large-scale galaxy distribution in the southern sky redshift survey. *Astrophysical Journal*, 390:17, May 1992. doi: 10.1086/171255.

Kevin M McLin, John T Stocke, R. J Weymann, Steven V Penton, and J. Michael Shull. The local ly forest: Absorbers in galaxy voids. *The Astrophysical Journal*, 574:L115, Aug 2002. doi: 10.1086/342419.

V Müller, S Arbabi-Bidgoli, J Einasto, and D Tucker. Voids in the las campanas redshift survey versus cold dark matter models. *Monthly Notices of the Royal Astronomical Society*, 318:280, Oct 2000. doi: 10.1046/j.1365-8711.2000.03775.x.

Mark C Neyrinck. Zobov: a parameter-free void-finding algorithm. *Monthly Notices of the Royal Astronomical Society*, 386:2101, Jun 2008. doi: 10.1111/j.1365-2966.2008.13180.x. (c) Journal compilation © 2008 RAS.

Yookyung Noh and J. D Cohn. The geometry of the filamentary environment of galaxy clusters. *Monthly Notices of the Royal Astronomical Society*, 413:301, May 2011. doi: 10.1111/j.1365-2966.2010.18137.x.

Danny C Pan, Michael S Vogeley, Fiona Hoyle, Yun-Young Choi, and Changbom Park. Cosmic voids in sloan digital sky survey data release 7. *arXiv*, astro-ph.CO, Mar 2011. 10 pages.

Changbom Park, Yun-Young Choi, Michael S Vogeley, J. Richard Gott, and Michael R Blanton. Environmental dependence of properties of galaxies in the sloan digital sky survey. *The Astrophysical Journal*, 658:898, Apr 2007. doi: 10.1086/511059.

Daeseong Park and Jounghun Lee. Void ellipticity distribution as a probe of cosmology. *Physical Review Letters*, 98:81301, Feb 2007. doi: 10.1103/PhysRevLett.98.081301.

S. G Patiri, J Betancort-Rijo, and F Prada. On an analytical framework for voids: their abundances, density profiles and local mass functions. *Monthly Notices of the Royal Astronomical Society*, 368: 1132, May 2006a. doi: 10.1111/j.1365-2966.2006.10202.x.

Santiago G Patiri, Francisco Prada, Jon Holtzman, Anatoly Klypin, and Juan Betancort-Rijo. The properties of galaxies in voids. *Monthly Notices of the Royal Astronomical Society*, 372:1710, Nov 2006b. doi: 10.1111/j.1365-2966.2006.10975.x.

P. J. E Peebles. The void phenomenon. *The Astrophysical Journal*, 557:495, Aug 2001. doi: 10.1086/322254. (c) 2001: The American Astronomical Society.

P. S Pellegrini, L. N da Costa, and R. R de Carvalho. Voids in the southern galactic cap. *Astrophysical Journal*, 339:595, Apr 1989. doi: 10.1086/167320.

Will J Percival, Beth A Reid, Daniel J Eisenstein, Neta A Bahcall, Tamas Budavari, Joshua A Frieman, Masataka Fukugita, James E Gunn, Željko Ivezić, Gillian R Knapp, Richard G Kron, Jon Loveday, Robert H Lupton, Timothy A McKay, Avery Meiksin, Robert C Nichol, Adrian C Pope, David J Schlegel, Donald P Schneider, David N Spergel, Chris Stoughton, Michael A Strauss, Alexander S Szalay, Max Tegmark, Michael S Vogeley, David H Weinberg, Donald G York, and Idit Zehavi. Baryon acoustic oscillations in the sloan digital sky survey data release 7 galaxy sample. *Monthly Notices of the Royal Astronomical Society*, 401:2148, Feb 2010. doi: 10.1111/j.1365-2966.2009.15812.x.

Massimo Persic and Paolo Salucci. Galaxy rotation curves: Dynamical signatures of the disk and the halo. *Astrophysical Letters and Communications*, 28:307, Jan 1992.

Erwin Platen, Rien van de Weygaert, and Bernard J. T Jones. Alignment of voids in the cosmic web. *Monthly Notices of the Royal Astronomical Society*, 387:128, Jun 2008. doi: 10.1111/j.1365-2966.2008.13019.x. (c) Journal compilation © 2008 RAS.

Manolis Plionis and Spyros Basilakos. The size and shape of local voids. *Monthly Notices of the Royal Astronomical Society*, 330:399, Feb 2002. doi: 10.1046/j.1365-8711.2002.05069.x.

C. C Popescu, U Hopp, and H Elsaesser. Results of a search for emission-line galaxies towards nearby voids. the spatial distribution. *Astronomy and Astrophysics*, 325:881, Sep 1997.

Michael Rauch, Wallace L. W Sargent, and Tom A Barlow. Small-scale structure at high redshift. i. glimpses of the interstellar medium at redshift 3.5. *The Astrophysical Journal*, 515:500, Apr 1999. doi: 10.1086/307060.

Eniko Regos and Margaret J Geller. The evolution of void-filled cosmological structures. *Astrophysical Journal*, 377:14, Aug 1991. doi: 10.1086/170332.

Randall R Rojas, Michael S Vogeley, Fiona Hoyle, and Jon Brinkmann. Photometric properties of void galaxies in the sloan digital sky survey. *The Astrophysical Journal*, 617:50, Dec 2004. doi: 10.1086/425225. (c) 2004: The American Astronomical Society.

Randall R Rojas, Michael S Vogeley, Fiona Hoyle, and Jon Brinkmann. Spectroscopic properties of void galaxies in the sloan digital sky survey. *The Astrophysical Journal*, 624:571, May 2005. doi: 10.1086/428476. (c) 2005: The American Astronomical Society.

H. J Rood. Voids. *IN: Annual review of astronomy and astrophysics. Volume 26 (A89-14601 03-90). Palo Alto*, 26:245, Jan 1988. doi: 10.1146/annurev.aa.26.090188.001333.

Barbara S Ryden. Measuring q 0 from the distortion of voids in redshift space. *Astrophysical Journal v.452*, 452:25, Oct 1995. doi: 10.1086/176277.

Barbara S Ryden and Adrian L Melott. Voids in real space and in redshift space. *Astrophysical Journal v.470*, 470:160, Oct 1996. doi: 10.1086/177857.

Varun Sahni, B. S Sathyaprakash, and Sergei F Shandarin. Shapefinders: A new shape diagnostic for large-scale structure. *Astrophysical Journal Letters v.495*, 495:L5, Mar 1998. doi: 10.1086/311214. (c) 1998: The American Astronomical Society.

W Saunders, W. J Sutherland, S. J Maddox, O Keeble, S. J Oliver, M Rowan-Robinson, R. G McMahon, G. P Efstathiou, H Tadros, S. D. M White, C. S Frenk, A Carramiñana, and M. R. S Hawkins. The pscz catalogue. *Monthly Notices of the Royal Astronomical Society*, 317:55, Sep 2000. doi: 10.1046/j.1365-8711.2000.03528.x.

W. E Schaap and R van de Weygaert. Continuous fields and discrete samples: reconstruction through delaunay tessellations. *Astronomy and Astrophysics*, 363:L29, Nov 2000.

Sergei Shandarin, Hume A Feldman, Katrin Heitmann, and Salman Habib. Shapes and sizes of voids in the lambda cold dark matter universe: excursion set approach. *Monthly Notices of the Royal Astronomical Society*, 367:1629, Apr 2006. doi: 10.1111/j.1365-2966.2006.10062.x.

Sergei F Shandarin. Nonlinear dynamics of the large-scale structure in the universe. *Physica D: Nonlinear Phenomena*, 77:342, Oct 1994. doi: 10.1016/0167-2789(94)90144-9.

Stephen A Shectman, Stephen D Landy, Augustus Oemler, Douglas L Tucker, Huan Lin, Robert P Kirshner, and Paul L Schechter. The las campanas redshift survey. *Astrophysical Journal v.470*, 470:172, Oct 1996. doi: 10.1086/177858.

Ravi K Sheth and Rien van de Weygaert. A hierarchy of voids: much ado about nothing. *Monthly Notices of the Royal Astronomical Society*, 350:517, May 2004. doi: 10.1111/j.1365-2966.2004.07661.x.

Ramin Skibba, Ravi K Sheth, Andrew J Connolly, and Ryan Scranton. The luminosity-weighted or 'marked' correlation function. *Monthly Notices of the Royal Astronomical Society*, 369:68, Jun 2006. doi: 10.1111/j.1365-2966.2006.10196.x.

Ramin A Skibba and Ravi K Sheth. A halo model of galaxy colours and clustering in the sloan digital sky survey. *Monthly Notices of the Royal Astronomical Society*, 392:1080, Jan 2009. doi: 10.1111/j.1365-2966.2008.14007.x.

E Slezak, V de Lapparent, and A Bijaoui. Objective detection of voids and high-density structures in the first cfa redshift survey slice. *Astrophysical Journal*, 409:517, Jun 1993. doi: 10.1086/172683.

Britton D Smith, Eric J Hallman, J. Michael Shull, and Brian W O'Shea. The nature of the warm/hot intergalactic medium i. numerical methods, convergence, and ovi absorption. *eprint arXiv*, 1009:261, Sep 2010.

D. N Spergel, R Bean, O Doré, M. R Nolta, C. L Bennett, J Dunkley, G Hinshaw, N Jarosik, E Komatsu, L Page, H. V Peiris, L Verde, M Halpern, R. S Hill, A Kogut, M Limon, S. S Meyer, N Odegard, G. S Tucker, J. L Weiland, E Wollack, and E. L Wright. Three-year wilkinson microwave anisotropy probe (wmap) observations: Implications for cosmology. *The Astrophysical Journal Supplement Series*, 170:377, Jun 2007. doi: 10.1086/513700.

Volker Springel. The cosmological simulation code gadget-2. *Monthly Notices of the Royal Astronomical Society*, 364:1105, Dec 2005. doi: 10.1111/j.1365-2966.2005.09655.x.

John T Stocke, Charles W Danforth, J. Michael Shull, Steven V Penton, and Mark L Giroux. The metallicity of intergalactic gas in cosmic voids. *The Astrophysical Journal*, 671:146, Dec 2007. doi: 10.1086/522920.

Michael A Strauss, Amos Yahil, Marc Davis, John P Huchra, and Karl Fisher. A redshift survey of iras galaxies. v - the acceleration on the local group. *Astrophysical Journal*, 397:395, Oct 1992. doi: 10.1086/171796.

Michael A Strauss, David H Weinberg, Robert H Lupton, Vijay K Narayanan, James Annis, Mariangela Bernardi, Michael Blanton, Scott Burles, A. J Connolly, Julianne Dalcanton, Mamoru Doi, Daniel Eisenstein, Joshua A Frieman, Masataka Fukugita, James E Gunn, Željko Ivezić, Stephen Kent, Rita S. J Kim, G. R Knapp, Richard G Kron, Jeffrey A Munn, Heidi Jo Newberg, R. C Nichol, Sadanori Okamura, Thomas R Quinn, Michael W Richmond, David J Schlegel, Kazuhiro Shimasaku, Mark SubbaRao, Alexander S Szalay, Dan Vanden Berk, Michael S Vogeley, Brian Yanny, Naoki Yasuda, Donald G York, and Idit Zehavi. Spectroscopic target selection in the sloan digital sky survey: The main galaxy sample. *The Astronomical Journal*, 124:1810, Sep 2002. doi: 10.1086/342343.

Ryuichi Takahashi, Naoki Yoshida, Takahiko Matsubara, Naoshi Sugiyama, Issha Kayo, Takahiro Nishimichi, Akihito Shirata, Atsushi Taruya, Shun Saito, Kazuhiro Yahata, and Yasushi Suto. Simulations of baryon acoustic oscillations - i. growth of large-scale density fluctuations. *Monthly Notices of the Royal Astronomical Society*, 389:1675, Oct 2008. doi: 10.1111/j.1365-2966.2008.13731.x.

Trinh X Thuan, J. Richard Gott, and Stephen E Schneider. The spatial distribution of dwarf galaxies in the cfa slice of the universe. *Astrophysical Journal*, 315:L93, Apr 1987. doi: 10.1086/184867.

A. V Tikhonov. Properties of voids in the 2dfgrs galaxy survey. *Astronomy Letters*, 32:727, Nov 2006. doi: 10.1134/S1063773706110028.

A. V Tikhonov. Voids in the sdss galaxy survey. *Astronomy Letters*, 33:499, Aug 2007. doi: 10.1134/S1063773707080014.

Anton V Tikhonov and Anatoly Klypin. The emptiness of voids: yet another overabundance problem for the cold dark matter model. *Monthly Notices of the Royal Astronomical Society*, 395:1915, Jun 2009. doi: 10.1111/j.1365-2966.2009.14686.x.

Jeremy L Tinker and Charlie Conroy. The void phenomenon explained. *The Astrophysical Journal*, 691:633, Jan 2009. doi: 10.1088/0004-637X/691/1/633.

R van de Weygaert and E van Kampen. Voids in gravitational instability scenarios - part one - global density and velocity fields in an einstein - de-sitter universe. *R.A.S. MONTHLY NOTICES V.263*, 263:481, Jul 1993.

Matteo Viel, Jörg M Colberg, and T.-S Kim. On the importance of high-redshift intergalactic voids. *Monthly Notices of the Royal Astronomical Society*, 386:1285, May 2008. doi: 10.1111/j.1365-2966.2008.13130.x.

Alexander M von Benda-Beckmann and Volker Müller. Void statistics and void galaxies in the 2df galaxy redshift survey. *Monthly Notices of the Royal Astronomical Society*, 384:1189, Mar 2008. doi: 10.1111/j.1365-2966.2007.12789.x.

David H Weinberg, Jordi Miralda-Escude, Lars Hernquist, and Neal Katz. A lower bound on the cosmic baryon density. *Astrophysical Journal v.490*, 490:564, Dec 1997. doi: 10.1086/304893.

Donald G York, J Adelman, John E Anderson, Scott F Anderson, James Annis, Neta A Bahcall, J. A Bakken, Robert Barkhouser, Steven Bastian, Eileen Berman, William N Boroski, Steve Bracker, Charlie Briegel, John W Briggs, J Brinkmann, Robert Brunner, Scott Burles, Larry Carey, and Michael A Carr. The sloan digital sky survey: Technical summary. *The Astronomical Journal*, 120:1579, Sep 2000. doi: 10.1086/301513.

Naoki Yoshida, Ravi K Sheth, and Antonaldo Diaferio. Non-gaussian cosmic microwave background temperature fluctuations from peculiar velocities of clusters. *Monthly Notices of the Royal Astronomical Society*, 328:669, Dec 2001. doi: 10.1046/j.1365-8711.2001.04899.x.

Zheng Zheng and David H Weinberg. Breaking the degeneracies between cosmology and galaxy bias. *The Astrophysical Journal*, 659:1, Apr 2007. doi: 10.1086/512151.

Vita

Danny Chia-Yu Pan was born in Taipei, Taiwan in 1982. His family immigrated to the United States of America in 1989 and he received his US citizenship in 1997. He spent the majority of his life growing up in the Washington D.C. area, attending Montgomery Blair High School. He graduated with double degrees from the University of Maryland, College Park in 2004, with a Bachelor of Science in Computer Science, and a Bachelor of Science in Astronomy. He did his graduate work at Drexel University, receiving a Masters of Science in Physics in 2008, and finishing his Doctorate in Philosophy in 2011.